Optimization of The Energy Systems of Residential Buildings

Using PV, Heat Pump and Battery Technology

Tekin Kodzhabash

Delft University of Technology

TU Delft

Optimization of The Energy Systems of Residential Buildings

Using PV, Heat Pump and Battery Technology

by

Tekin Kodzhabash

Student Name	Student Number
Tekin Kodzhabash	5633192

Supervisor:	Rudi Santbergen
Daily Supervisor:	Youri Blom
Internal Committee Member:	Olindo Isabella
External Committee Member:	Sebastian Rivera Iunnissi
Faculty:	EEMC, Delft
Program:	Sustainable Energy Technology

To be defended publicly on Tuesday, January 30, 2024, at 14:00

TU Delft

Abstract

This thesis addresses the imperative need for sustainable energy solutions in the residential sector which is a significant contributor to global energy consumption and greenhouse gas emissions. Focusing on modeling and optimizing residential energy systems, the study explores the integration of photovoltaic (PV) panels, heat pumps, and batteries. The purpose is extending the applications of the Photovoltaic Material and Devices (PVMD) toolbox, offering a framework for future research and advancements. The objective is to enhance energy efficiency, reduce carbon footprints, and contribute to energy security by diversifying energy sources.

The research encompasses a comprehensive analysis of heat pump models, emphasizing their role in space heating, space cooling, and domestic hot water functions. Two specific models are chosen for Coefficient of Performance (COP) and Energy Efficiency Ratio (EER) calculations. These models, along with the utilization of the nPro tool, lay the foundation for integrating heat pump systems with PV production and battery storage in residential buildings.

The study successfully integrates the model of the battery's performance and the overall grid-connected energy system. Employing a mathematical modeling approach, each component is systematically incorporated into the system, including the previously developed heat pump model. This integration, coupled with the Alternating Current (AC) output of the PVMD toolbox and the battery, establishes the groundwork for subsequent economic and performance analyses of the system.

The study systematically selects various locations with different environmental conditions such as Equivalent Sun Hours (ESH) and average ambient temperature to analyze the economic aspect by checking the Net Present Cost (NPC) and performance aspects by checking Self Consumption Ratio (SCR) and Self Sufficiency Ratio (SSR) of the integration model. The findings emphasize the economic viability of heat pump investments in cities with distinct heating and cooling demands. It has been demonstrated that in colder cities where heating demand is predominant, heat pumps are economically attractive, resulting having heat pumps in optimal scenarios that give the minimum NPC in Amsterdam and Lisbon. Additionally, although the individual components of the system may seem cost-ineffective, their value is derived more from integration in milder cities where heating demand is dominant, resulting having heat pump and PV integrated for the optimal scenario for Lisbon. However, cities dominated by cooling demand face challenges in achieving financially optimal designs because the operational savings for cooling cannot be accurately included such as Cairo and Dakar. The research underscores the importance of considering various system factors, including initial investment costs and electricity tariffs, to achieve financially optimal sizing. As the initial cost of the battery decreases, battery technology becomes economically appealing for Lisbon and Dakar. Moreover, changes in the tariff prove economically favorable for integrating the battery system in Lisbon, Cairo, and Dakar.

This work contributes valuable insights to the field of renewable energy, providing practical solutions for the transition towards cleaner and more efficient residential energy systems.

Acknowledgement

With completing this project in Photovoltaic Material and Devices group that I have been working on during the past year, I am finalizing my journey of Master of Science in Sustainable Energy Technology program at Delft University of Technology.

I would like to express my gratitude to all the members of PVMD group for fostering a professional atmosphere and providing valuable guidance throughout my project. Special thanks go to my supervisors, Dr. ir. Rudi Santbergen and Youri Blom, without whom the successful completion of this project would not have been possible. Throughout the one year duration, they consistently made themselves available to share their expertise, address my inquiries, and offer constructive feedback. Moreover, their ability to inspire and keep me motivated played a crucial role in the project's success. I'm also very thankful to Prof.Dr.ir. Olindo Isabella and Dr. Sebastian Rivera Iunnissi for being part of my thesis committee.

I am deeply grateful for the enriching experience this master's program has provided me. Beyond the knowledge gained, it has gifted me with a sense of community, turning acquaintances into a second family. My heartfelt thanks extend to the wonderful individuals in the 'Ravers van Delft' and 'The Italians & Co.' groups; your presence has made this journey truly special

Throughout the twists and turns of this academic venture, I've been fortunate to share both challenges and triumphs with a remarkable group of friends. While the list is extensive, special appreciation goes to Dilara, Lucas, Penelope, Pierina, Clarissa, Tutku, Amaç, Yaren, Ebru, Haydar, and Eylül for their unwavering support.

Finally, my deepest and most sincere thanks are reserved for my parents. Without their boundless support, achieving this milestone would have been an insurmountable task. I am profoundly fortunate and grateful to be their child.

Tekin Kodzhabash
Delft, January 2024

Contents

Nomenclature

Abbreviations

Abbreviation	Definition
GHG	Greenhouse Gas
EU	European Union
PV	Photovoltaic
DC	Direct Current
AC	Alternating Current
PVMD	Photovoltaic Materials and Devices
CdTe	Cadmium Telluride
CIGS	Copper Indium Gallium Selenide
CPV	Concetrated Photovoltaic
COP	Coefficient of Performance
EER	Energy Efficiency Ratio
ASHP	Air Source Heat Pump
GSHP	Ground Source Heat Pump
WSHP	Water Source Heat Pump
SAHP	Solar Assisted Heat Pump
GCHP	Ground Coupled Heat Pump
DX-GSHP	Direct Expansion Ground Source Heat Pump
DX-SAHP	Direct Expansion Solar Assisted Heat Pump
IX-SAHP	Indirect Expansion Solar Assisted Heat Pump
BESS	Battery Energy Storage System
LA	Lead Acid
Li-Ion	Lithium İon
NaS	Sodium Sulphur
NaNiCl	Sodium Nickel Chloride
RFB	Redox Flow Battery
HFB	Hybrid Flow Battery
SOC	State of Charge
NPC	Net Present Cost
SCR	Self Consumption Rate
SSR	Self Sufficiency Rate

Symbols

Symbol	Definition	Unit
Q_L	Extracted heat	[kWh]
Q_H	Transferred heat	[kWh]
W	Work done at compressor	[kWh]
T_H	Heat source temperature	[K]
T_L	Heat exhaust temperature	[K]
T_{sink}	Sink side temperature	[C]
T_{source}	Source side temperature	[C]
T_g	Ground temperature	[C]
T_amb	Ambient air temperature	[C]

Symbol	Definition	Unit
a	Albedo number	[-]
GHI	Global horizontal irradiance	[W/m^2]
WS	Wind speed	[m/s]
T_w	Water temperature	[C]
$T_{sink,rad}$	Radiator supply temperature [C]	
$T_{sink,floor}$	Underfloor heating supply temperature [C]	
C_n	Battery capacity	[kWh]
P_{ch}	Charging power	[kW]
P_{dsch}	Discharging power	[kW]
t_{ch}	Charging time	[h]
t_{dsch}	Discharging power	[h]
$E_{pv,ac}$	AC PV energy	[kWh]
E_{bought}	Energy bought from the grid	[kWh]
E_{dch}	Discharged energy of BESS	[kWh]
$E_{consumed}$	Energy consumed by the house	[kWh]
E_{sold}	Energy sold to the grid	[kWh]
E_{ch}	Charging energy of battery	[kWh]
I_{pv}	Initial cost of PV	[€]
I_{hp}	Initial cost of heat pump	[€]
I_{bt}	Initial cost of battery	[€]
C_{ele}	Annual cost of electricity	[€]
C_{boiler}	Annual cost of natural gas	[€]
C_n	Total annual cost	[€]
e_{ele}	inflation rate of electricity	[-]
e_{eng}	inflation rate of natural gas	[-]
M	Initial cost fraction for maintenance	[-]
Ins	Initial cost fraction for insurance	[-]
d	discount rate	[-]
g	general inflation rate	[-]
η	Carnot efficiency	[-]
η_{ch}	Charging efficiency	[-]
η_{dsch}	Discharging efficiency	[-]
$\eta_{round-trip}$	Round-trip efficiency	[-]

1

Motivation and Background

The residential sector plays a crucial role in the overall consumption of global energy and is a significant source of greenhouse gas emissions(GHG). In fact, in the European Union (EU), the residential sector alone accounts for 25.4% of final energy consumption and contributes to 20% of the total GHG emissions [30]. This underscores the pressing need for energy-efficient solutions in residential buildings, especially in light of climate change and the urgent imperative to reduce carbon emissions. Furthermore, ensuring energy security, which refers to the reliable and uninterrupted access to energy, has become increasingly critical. The integration of renewable sources such as photovoltaic (PV) panels, heat pumps, and batteries into energy system of residential buildings not only aids in reducing carbon footprints and energy bills but also contributes to enhancing energy security by diversifying the energy mix and reducing dependency on traditional, often non-renewable sources.

The energy systems of residential buildings typically rely on grid-supplied electricity, which is often generated from non-renewable sources like fossil fuels. Moreover, the heating of the residential buildings mostly depend on the natural gas. This dependence on non-renewable energy sources adds more and more to GHG everyday. Given the urgency to achieve emissions reduction goals within tight timelines, the most rapid method for decarbonizing buildings is through the electrification of heat[16] and becoming less grid dependent.To address this issue, this thesis aims to model and optimize the performance of a residential energy system using PV panels, heat pumps, and batteries.

This research is significant because it addresses the need for sustainable and efficient energy systems in residential buildings. By optimizing the performance of these systems, it can be seen that if there is any favorable change for the homeowners in terms of energy bills and the system can be analyzed if there is a change about its carbon footprint. So, this changes can result in decreasing the overall GHG. Furthermore, this research will contribute to the development of innovative solutions for the growing demand for sustainable energy systems. The results of this research will also be useful for policy makers and industry professionals in the field of renewable energy. The research findings may inform the development of policies and programs aimed at promoting the adoption of renewable energy systems in residential buildings. Overall, the research is expected to make a valuable contribution to the field of renewable energy and sustainability.

Chapter 1 begins with an introduction to the topic and underscores the research's significance. Subsequently, a detailed review of each technology is provided. The literature on integrated systems, encompassing these technologies for residential buildings, is then presented. Finally, the study's intended contribution to filling knowledge gaps is explained, and the sequential goals of this thesis are outlined.

1.1. PV Technology

Photovoltaic (PV) technology has been increasingly used in recent years as a source of renewable energy in residential buildings. It is expected to increase even more in the future years, that 1081 GW

electricity is expected to be supplied by solar power[28]. This is related to the advantages of the technology provides. PV is regarded as the most viable renewable energy option suitable for implementation in residential settings, both as distributed systems and integrated into buildings. The performance of the system can be readily simulated based on solar radiation, taking into account the orientation of the panels by considering the azimuth and tilt angles[19]. PV technologies serve as a secure energy source that is clean and environmentally friendly. Studies examining the life cycle assessment of PV systems and a range of established and emerging technologies reveal that PV systems have a low environmental impact, with greenhouse gas emissions of about 0.043 kg CO2 eq/kWh. This positions PV systems as among the most environmentally friendly options when compared to traditional energy sources[19].

PV technology efficiently converts sunlight into electricity without relying on a heat engine. Each PV cell consists of layers of semiconductor material. When light interacts with the cell, generating an electric field, producing electricity through various semiconductor layers. The amount of electricity generated is determined by the light intensity hitting the cell. The PV cell generates the direct current (DC) first and then this energy can be converted to alternating current (AC) to be stored for later use. In evaluating a material's potential for application in PV, the band gap stands out as a crucial parameter. This parameter signifies the minimum energy required to elevate an electron in a semiconductor to a higher energy state. Only photons with energy equal to or greater than a material's band gap can be absorbed. In the context of solar cells, which produce power as the product of current and voltage, the band gap plays a pivotal role. While larger band gaps result in higher achievable voltages, they come at the expense of reduced sunlight absorption and, consequently, reduced current. This inherent trade-off implies that only a select group of materials possessing band gaps within an optimal range hold promise for effective use in PV [38]. In the fabrication of PV cells, silicon and similar semiconductor materials are utilized. By introducing impurities into the crystal lattice, the conductivity of the semiconductor can be readily adjusted, rendering it suitable for PV applications [28].

Solar cells come in various types, with wafer-based silicon cells dominating the market, constituting 90% of solar cells [28]. The main silicon materials utilized in the production of solar cells encompass single-crystalline, multicrystalline, and amorphous silicon. Additionally, other materials such as copper–indium–gallium–selenide (CIGS), cadmium–telluride (CdTe) and copper–indium–gallium–sulphide (CIGS2) are also employed. These cells can be categorized with three generations considering the manufacturing material and the level of commercial maturity.

The first-generation solar cell utilized silicon wafers, marking the oldest yet most widely adopted technology due to its high power efficiencies. In contrast, the technologies using thin-film PV, which are second-generation solar cells, encompass different families: amorphous silicon, micromorph silicon, CIGS and CdTe. Compared to the first-generation silicon wafer solar cells, these second-generation cells are more economically efficient. Thin-film polycrystalline silicon solar cells within this category can achieve power conversion efficiencies exceeding 19%, thanks to light trapping and back surface passivation. Moving to the third generation, solar cells in this category, such as concentrating PV (CPV) and organic PV cells, are still in the demonstration and research phase[28].

1.1.1. PVMD Toolbox

This project aims to extend the functionality of the PVMD Toolbox, a software tool introduced by the Photovoltaic Materials and Devices (PVMD) research group at Delft University of Technology for modeling and predicting the energy output of photovoltaic systems [40]. The toolbox is used to get the solar output for the integration model in this project.

The toolbox is divided into different models that run sequentially. It starts with the absorption model, followed by the ray tracing model and irradiance model. Additionally, the semiconductor model runs separately. The irradiance model is followed by the thermal model to track the cell temperature. The photo-generated current from the irradiance model is combined with the semiconductor and thermal models to execute the electrical model, providing the direct current output of the panels. Finally, the conversion model is run to obtain the ultimate output, which is the alternating current of the panels.

1.2. Heat Pump Technology

In recent years, heat pumps have become increasingly popular as an energy-efficient and environmentally friendly alternative to traditional heating systems. Given the increasing focus on curbing greenhouse gas emissions and shifting to renewable energy sources, heat pumps offer an appealing solution for residential buildings. Moreover, one of the most hopeful technologies to improve system efficiency and achieve the European energy and climate targets for 2030 and 2050 is the incorporation of heat pumps into district heating [34].

One of the main advantages of heat pumps is their ability to be integrated with renewable energy systems, such as solar or wind power. By using electricity to transfer heat, rather than burning fossil fuels, heat pumps can significantly reduce carbon emissions and help to create a more sustainable future.

In addition to their environmental benefits, heat pumps can also offer significant cost savings over the long term. While the initial installation costs of a heat pump system may be higher than those of a traditional heating system, the energy savings over time can more than make up for this initial investment. As per the U.S. Department of Energy, heat pumps have the potential to decrease energy consumption and related costs by up to 50% when compared to conventional heating systems[8].

Moreover, heat pumps provide a way better alternative than natural gas usage, which is still a common heating source in many residential buildings. Being a fossil fuel, natural gas contributes to greenhouse gas emissions and plays a role in climate change. Furthermore, prices of natural gas can be unpredictable and susceptible to market fluctuations. Heat pumps, on the other hand, provide a reliable and sustainable heating solution that is not subject to market volatility.

In conclusion, heat pumps offer a range of benefits for residential buildings, including their ability to integrate with renewable energy systems, their energy efficiency and cost savings, and their environmental advantages compared to traditional heating systems. With the continued focus on minimizing carbon emissions and shift towards renewable energy sources, heat pumps are likely to become an increasingly important component of residential energy systems in the coming years.

1.2.1. Basic Working Principle of Heat Pumps

At its core, a heat pump is an electrically powered device that operates by absorbing heat from a source side that is low-temperature and transferring it to a higher-temperature sink.[10] Heat naturally flows from locations with higher temperatures to those with lower temperatures, but by utilizing the principles of thermodynamics, a heat pump can effectively reverse this process, cooling the low-temperature side while heating the high-temperature side.

The fundamental elements of a heat pump consist of the refrigerant, serving as the working fluid, condenser (inside coil), expansion valve, evaporator (outside coil) and compressor. The components and the schematic of the heat pump can be seen as in Figure 1.1.

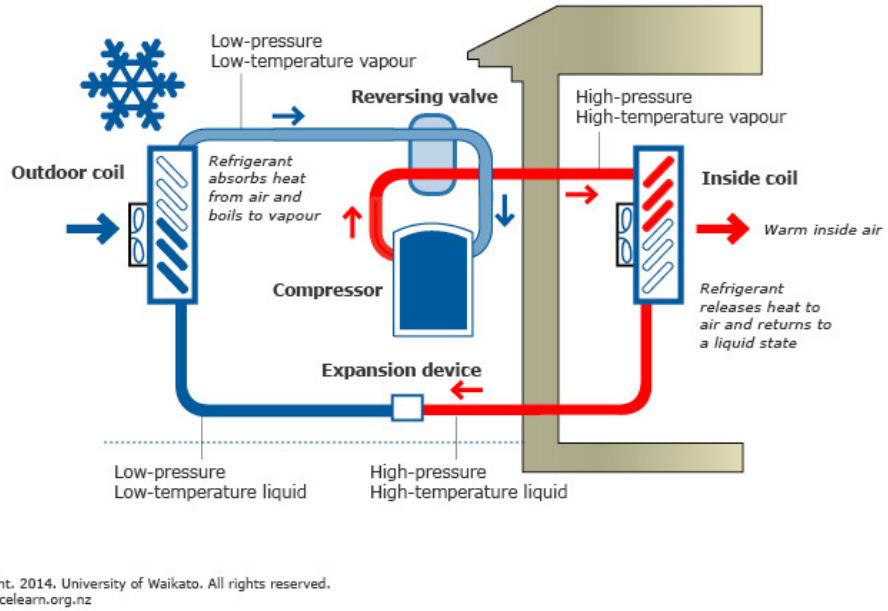

Figure 1.1: Basic components and the schematic of a heat pump.[12]

A four-stage cycle summarizes the operation of the heat pump. Those cycles include compression and expansion using the pumps, and evaporation and condensation using the heat exchangers. During the cycle, the refrigerant absorbs heat from the source, which causes it to undergo a phase change. Afterward, the reversal of the phase change occurs, and the heat is conveyed to the sink, which could be air or water employed for heating space and hot water. Furthermore, a four-way valve allows the refrigerant flow to be inverted, allowing the heat pump to take in warmth from an internal area and transfer it to the external sink, facilitating space cooling.

The basic principles governing the refrigeration cycle for heating space are outlined as follows: [42]:

- Initially, during the compression phase, the refrigerant is compressed in its vapor state, resulting in an increase in both temperature and pressure.
- In the condensation part, the vapour refrigerant that is high in pressure and temperature goes to the condenser, where the sink receives the heat transfer. The refrigerant transforms into a liquid state. However, it remains at high temperature and pressure.
- As the refrigerant passes through an expansion valve, the pressure and temperature are lowered in the expansion stage.
- Finally, in the evaporation part, the liquid refrigerant absorbs heat from the source, and transforms into a cold vapour refrigerant. The refrigerant then returns to the compressor to initiate the subsequent cycle.

The following equations are the core equations to understand the working principle of the heat pumps and evaluate the performance of them.

$$Q_L + W = Q_H \tag{1.1}$$

where Q_L is leaving the source as the extracted heat, Q_H is going to the sink side as the transferred heat and W is the work done at the compressor.

In heat pumps, the most important parameters to characterize the system are Coefficient of Performance (COP) and Energy Efficiency Ratio (EER), that are the ratios of the heat flow of interests to the

works needed to be done at the compressor. COP can be defined for heating and EER for cooling cycles as follows:

$$COP = \frac{Q_H}{W} = \frac{Q_L + W}{W} \tag{1.2}$$

$$EER = \frac{Q_L}{W} \tag{1.3}$$

Even though it is less relevant to heat pumps, the Carnot efficiency can be defined as:

$$\eta = \frac{W}{Q_H} = \frac{Q_H - Q_L}{Q_H} = 1 - \frac{Q_L}{Q_H} = 1 - \frac{T_L}{T_H} \tag{1.4}$$

where, T_H represents the temperature of the engine's heat source, and T_L corresponds to the temperature of the low-temperature exhaust, both measured in Kelvin.

1.2.2. Classification of Heat Pumps

Heat pumps come in various types, each with its unique features and applications. The type of the heat pump selection changes with various factors such as the desired output temperature, heat source, and environmental conditions. In this chapter, we will discuss the most commonly used types of heat pumps for residential purposes [42], including Air Source Heat Pump(ASHP), Water Source Heat Pump(WSHP), Ground Source Heat Pump(GSHP), Solar Assisted Heat Pump(SAHP), Cascade Heat Pump, and Two-Stage Heat Pumps. By understanding the different types of heat pumps and their features, one can make an informed decision about which heat pump type to choose for their specific residential needs.

Air Source Heat Pump (ASHP)

In ASHPs, the mentioned source in subsection 1.2.1 is air. Therefore, the heat is extracted from the air outside. Due to their easy operation, high performance, and favorable environmental properties, air source heat pumps have become a popular choice for heating, cooling, and domestic hot water heating [44]. In colder temperatures, the efficiency of ASHPs goes down as the ambient temperature decreases. This limitation arises from the constrained quantity of heat energy that the evaporator can extract from the surrounding air during winter. Additionally, the occurrence of frost poses a notable challenge in the selection of ASHPs. In the heating season, frost tends to develop regularly when the evaporator coil's surface temperature drops below 0 °C. [42]

ASHPs can be further categorized with two types based on the heat sink they use. In air-to-air heat pumps, the heat sink is the air, while air replaces with water for air-to-water type.

Water Source Heat Pump (WSHP)

The high density and specific heat capacity of water make it a desirable heat source and sink for heat pumps. Compared to air, water can hold more energy per volume and has a smaller temperature range. This is attributed to the notably higher density of water and its roughly fourfold greater specific heat capacity compared to air [42]. Water source heat pumps can be categorized into two types: water-to-water and water-to-air heat pumps.

Ground Source Heat Pump (GSHP)

The ground serves as a frequently employed source and reservoir of heat in heat pumps used for heating and cooling applications. This is because of its stable temperature, which remains relatively constant compared to the fluctuating temperatures of air. The ground is regarded as one of the most efficient and available renewable energy sources, owing to its eco-friendliness, long-lasting nature, ability to store energy, and availability throughout the day [42]. There are three types of ground source heat pumps: direct expansion ground source heat pumps(DX-GSHP), ground-coupled heat pumps(GCHP) and groundwater heat pumps.

In GCHP, the heat sink and source is the ground according to the heating and cooling mode, whereas groundwater heat pumps extract heat from a groundwater source. Ground-coupled heat pumps (GCHPs) use buried pipes called a ground loop to extract heat from the earth for winter heating or to reject heat to the ground for summer cooling. In contrast, the heat is extracted from a source of water like wells or pond for heating or reject heat to the water for cooling the building with groundwater heat pumps.

DX-GSHP system operates by directly circulating the refrigerant within the borehole heat exchanger, which transmits the heat to the surrounding soil. Essentially, the borehole heat exchangers serve as either an evaporator or a condenser, depending on the system's space cooling or heating mode [42].

Solar Assisted Heat Pump (SAHP)

Solar power can serve as the exclusive heat provider for heat pumps or can be combined with other sources like air and ground. The connection methods of the solar collector and evaporator lead to the categorization of SAHP into a direct expansion-solar assisted heat pump (DX-SAHP) and an indirect expansion solar-assisted heat pump (IX-SAHP) system [42].

Cascade Heat Pump

The cascade heat pump is a setup consisting of two refrigerant cycles—specifically, the low-stage and high-stage—connected through a cascade heat exchanger. This heat exchanger functions as a condenser in the low-stage cycle and as an evaporator in the high-stage cycle. Therefore, instead of two heat exchangers (evaporator and condenser), this system only has one. One significant benefit of the cascade heat pump is that it uses two distinct refrigerants within two different cycles, allowing them to operate under their ideal conditions [42].

Two-Stage Heat Pumps

Two-stage heat pumps are a feasible solution to address the decreased performance of conventional air source heat pumps (ASHPs) in cold climates [42]. The system consists of two compressors, two expansion valves, an evaporator coil, a sub-cooler, and a plate heat exchanger for producing hot water. The refrigerant discharged from the low-stage compressor, combined with the two-phase refrigerant from the sub-cooler, enters the high-stage compressor in a saturated vapor state. This process lowers the discharge temperature of the high-stage compressor. The rest of the condensed refrigerant from the plate heat exchanger undergoes supercooling through interaction with the two-phase refrigerant in the sub-cooler, thereby enhancing the COP of the system. This two-stage heat pump system can maintain the COP and heating capacity at low ambient temperatures, making it an ideal solution for cold climate regions.

Comparison of Different Heat Pump Types

The heat pump types discussed in the previous chapter can be summarized in terms of their advantages and disadvantages, taking into account practical and economic factors as can be seen in Table 1.1.

1.3. Battery Energy Storage Systems (BESS)

The integration of BESS technologies for residential buildings has gained a major attention in recent years, thanks to theirs potential to help reduce the reliance on the electrical grid and allow for more efficient use of energy generated from renewable sources such as solar panels.

Batteries used in residential buildings store excess electrical energy generated by the solar panels during the daytime for use during the night or on cloudy days when solar generation is low. By storing energy when it is plentiful and releasing it when needed, batteries can help mitigate the intermittency and variability of renewable energy sources, making it possible to more effectively use renewable energy to power homes [43].

With the increasing adoption of renewable energy sources, such as solar panels, the need for reliable and efficient energy storage solutions is growing everyday. The integration of battery technology provides an effective solution to this problem, allowing homeowners to store excess energy produced

Table 1.1: Comparison of different heat pumps.[42]

Heat Pumps	Pros	Cons
Air Source Heat Pump	Easy to operate and has a low installation cost	At low ambient temperatures frost formation occurs on the outside of the evaporator
	Consumes less primary energy and emits fewer greenhousegases compared to fossil-fuel based system	Lower heating capacity and COP under cold climates
Water Source Heat Pumps	Abundant sources such as ponds,lakes and rivers can be used as a heat source	Climate conditions affects the temperature of the surface water
	Higher COP and energy efficiency ratio than ASHPs	Heat exchanger can face corrosion, blockage, and fouling due to low water quality
		Water availability can limit the use of WSHP
Ground Source Heat Pumps	Higher COP and energy savings than ASHP	High installation costs and land requirement
	Better performance in colder climates	Antifreeze solutions and potential leak of refrigerant
	Significant GHG reductions compared to fossil-fuel based systems	Underground heat accumulation and depletion may affect the system
		Metal corrosion of GHEs
Solar Assisted Heat Pumps	Significant environment and economic benefits	Solar intermittency affects the system performance
	Higher-temperature heat being delivered to heat pumps	Complex control system
		Higher installation costs
Cascade Heat Pumps	Can work efficiently under cold climates	Higher installation costs
	Higher COP than single-stage heat pumps	Higher operating costs
	Great GHG emissions reduction compared to fossil-fuel based systems	Hard to add a four-way valve to achieve heating or cooling
Two Stage Heat Pumps	Higher COP and heating capacity than ASHP	Significantly higher costs than ASHP
	Better performance in cold climates	Complex control system

when there is high generation and use it whenever energy demand exceeds supply.

By effectively managing the energy generated by solar panels and storing it for use when needed, the integration of battery technology has the future to significantly lower the carbon footprint of residential buildings. This not only benefits individual homeowners but also contributes to the global effort to reduce GHG and take up arms climate change.

1.3.1. Different BESS Technologies

Batteries can be categorized into two main types that are secondary batteries and flow batteries. Secondary batteries are composed of cells, each containing two electrodes immersed in an electrolyte. They have the capability to store and supply energy through reversible electrochemical reactions. Typically, in these reactions, the anode or negative electrode undergoes oxidation, producing electrons, while the cathode or positive electrode undergoes reduction, accepting electrons through an external circuit connected to the cell terminals [22]. The secondary batteries are further categorized with various types, such as lead–acid, Li-ion, NiCd/NiMH, sodium–sulfur, metal–air, and sodium–nickel chloride.

Flow batteries systems possess the ability to store energy over extended periods, ranging from hours to days, exhibiting power capacities of several megawatts. Flow batteries are divided into further categories: redox flow batteries and hybrid flow batteries[4].

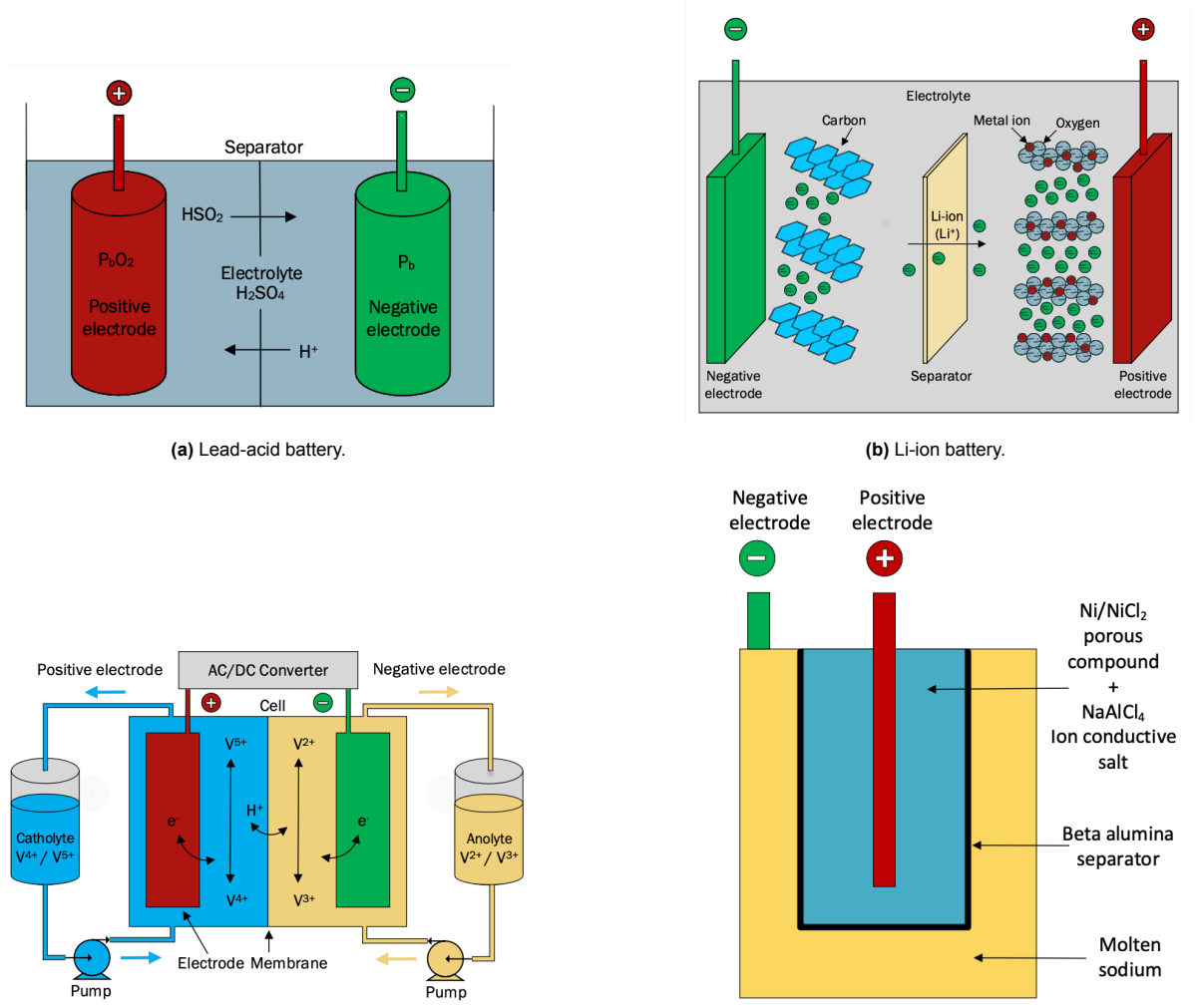

(a) Lead-acid battery.

(b) Li-ion battery.

(c) Redox Flow battery

(d) Sodium nickel chloride battery

Figure 1.2: Configuration and main components of some battery types[22].

Lead−Acid Battery (LA)

Lead–acid batteries, dating back to around 1890, stand as the most widely utilized battery type globally. They typically exhibit a service life ranging from 6 to 15 years, with 1500 cycles with efficiency of 80–90 % and at a certain percentage depth of discharge. However, drawbacks include low energy density and the use of lead, a hazardous material subject to prohibition and restriction in certain areas. On the positive side, lead–acid batteries offer a attracting cost/performance ratio, being recycled easily, and a straightforward charging method. Ongoing efforts in lead–acid battery development focus on enhancing efficiency, particularly for micro-hybrid electric vehicles [4].

Lithium-Ion Battery (Li-Ion)

In recent years, Li-Ion batteries have seen increased use in stationary power applications, leveraging experience from their development in electric and hybrid vehicles. Comprising positive and negative electrodes separated by porous polymeric materials in an electrolyte, these batteries use a metal ion (e.g., Co, Ni, Mn) and oxygen in the positive electrode and carbon materials like graphite in the negative electrode. Their key features include the highest energy density, making them suitable for various energy storage systems. They exhibit stable discharge voltage, operate in a wide temperature range, offer safety, and have a cycle efficiency around 85 %. Compared to aqueous battery technologies, they are lightweight with packaging flexibility, and their cathode material is low-cost and recyclable. Despite their benefits, lithium-ion batteries face challenges like internal resistance heating, requiring overcurrent and overvoltage systems for protection. This protection increases costs, and safety concerns arise if charge voltages are exceeded, leading to thermal runaway and potential hazards. The charging circuitry complexity and the need for individual cell monitoring are drawbacks, and there are concerns about resource availability for large-scale energy storage. Environmental issues include lithium's reactivity, flammability, and toxicity of some electrodes and electrolytes. Additionally, cycle depth of discharge can impact battery life, and their fragility is temperature-dependent [22].

Metal-Air Battery

A metal–air electrochemical cell comprises a pure metal anode and a cathode connected to a plentiful air supply, employing solely oxygen in the electrochemical process. The lithium air battery is attractive but poses safety risks due to lithium's reactivity. The zinc–air battery, with a practically feasible specific energy, is more viable currently. However, designing rechargeable zinc–air cells is challenging. Despite the potential for a cost-effective and high-specific-energy electrically rechargeable metal–air system, none have yet reached market viability[4].

Sodium-Sulphur Battery (NaS)

Employing a solid beta-alumina ceramic electrolyte, sodium–sulfur (NaS) batteries segregate the active components, featuring molten sodium at the cathode and molten sulfur at the anode. These batteries exhibit a discharge duration ranging from 6.0 to 7.2 hours and 4500 cycles of standard life. They are known for their efficiency and quick response. NaS batteries, despite lacking an inherent heat source, can effectively manage the heat generated during frequent use through appropriately sized insulation, utilizing the heat produced within the battery's own reaction. They prove particularly suitable for applications involving high-frequency cycling [4].

Sodium-Nickel Chloride Battery (NaNiCl)

The NaNiCl battery, commonly named as the ZEBRA battery, is a high-temperature (HT) battery introduced to the sector around 1995. Compared to NaS batteries, NaNiCl batteries exhibit superior safety, cell voltage, and tolerance to limited discharge and overload. Demonstrating effectiveness across diverse electric vehicle designs, these batteries are viewed as a feasible choice for fleet applications. Continuous advancements involve improved iterations of the ZEBRA battery, featuring heightened power density suitable for hybrid electric vehicles, and high-energy variants specifically designed for storing renewable power for load-leveling and industrial applications[4].

Redox Flow Battery (RFB)

In a redox flow battery, the positive and negative electrodes contain catholyte and anolyte electrolytes. During discharge, dissolved active masses continually supply the electrodes, with the converted product returning to the tank. Exchange of charge involves a current flow within electrodes, usable by

battery-powered devices. While redox flow batteries are explored for electric vehicles, their low electrolyte energy density remains a challenge. An RFB could be quickly recharged by draining and replacing the emptied electrolyte with refilled electrolyte[4].

Hybrid Flow Battery (HFB)
A HFB retains an active mass within the electrochemical cell and the other externally, combining some advantages of RFBs and classic secondary batteries. Examples of HFBs include the Zn-Br and Zn-Ce systems. Exxon took the lead in developing the Zn-Br hybrid flow battery in the beginning of 1970s, and currently, multiple companies are in the process of commercializing it. Additionally, there are continuous advancements, with ongoing developments focused on 5 kW/20 kWh community energy storage devices that leverage this technology [4].

1.4. Integrated Systems

The integration of photovoltaic (PV) technology, heat pumps, and batteries has been proposed as a promising solution for achieving highly energy efficient systems and sustainability in residential field. This subsection will review the relevant literature on the integration of these systems, highlighting the different approaches and techniques used in previous studies. The focus will be on the outcomes of these studies, with an emphasis on the key findings and contributions. By examining the current state of the art in integrated PV, heat pump, and battery systems, this subsection aims to provide a comprehensive understanding of the existing research and identify potential areas for further investigation.

One study, which concentrated on the cost-optimal sizing of a photovoltaic-battery combination and an air-water heat pump addition to cover the space cooling and heating purposes in Italy [21], revealed that the PV system size is contingent upon the thermal demands of the building. Additionally, the battery size is influenced by both the climate and the dimensions of the PV system. The study recommends an integrated sizing approach for the three systems. Another study proposed a Solar Plus system that optimizes distributed solar PV together with the BESS and dispatchable loads in residential buildings with smart air-conditoning unit and water heater using NREL optimization model for a generic house in the U.S[26]. The results showed that improved end-user economics are observed with the solar-plus approach across various rate structures, particularly for that pose challenges for solar, such as non-coincident time-of-use structures, lower grid export rates, and demand charges.

Another research work developed a predictive management system to build energy supply networks including PV system, heat pumps for water heating with a thermal storage tank, and batteries through two-stage stochastic programming and rule-based control [41]. The study found that The simulation results suggest a slight decrease in the annual operating cost reduction achieved by the developed management compared to the ideal management based on the previously known PV output. Furthermore, under conditions where the selling price of surplus PV output is higher, the developed management proves advantageous in annual operating cost compared to charging and exporting priority strategies. Another study focused on the interaction of PV panels of a house's rooftop combining an electric vehicle's battery storage and an air-to-water heat pump for space heating and cooling using TRNSYS simulation environment for the city of Volos [37]. According to the findings of this research, the potential combination of financial incentives for both electric vehicle purchase and rooftop PV installation in homeowners' residences shows great promise. This is attributed to the synergies observed between electrical storage and rooftop photovoltaic installations.

Furthermore, a suggested optimal strategy for operating, configuring, and sizing generation and storage technologies for residential heat pump systems has been outlined in one of the studies [3].The emphasis of this approach is on maximizing the self-consumption of photovoltaic electricity in the context of space heating and domestic hot water. The study found that the most effective configuration and operation of the system depended on a range of factors, including the size of the PV panels, the size of the heat pump, and respecting household's electricity consumption profile. Moreover, a research study delved into the electrification of houses' heating, cooling, and hot water by employing onsite PV, heat pumps, and thermal storage for load smoothing, utilizing TRNSYS simulation[16]. The study found that the system's optimal design and operation depended on the electricity and thermal demand profiles,

and with the control the grid dependency can be decreased while self consumption can be increased.

A particular study has conducted a techno-economic analysis of integrated combined heating, cooling, and power (CCHP) systems utilizing different renewable energy sources and storage units for residential applications, employing TRNSYS simulation.[1]. The findings suggest that the optimal design and operation of CCHP systems depend on various factors, including the energy demand, the availability of renewable energy sources, and the prices of electricity and gas. Another study proposed a sustainable polygeneration system for a residential building that integrates renewable energy sources, energy storage units, and a CCHP system [39]. The study demonstrated that the proposed system can significantly reduce energy consumption and CO_2 emissions.

Several studies have proposed reinforcement learning approaches for home energy management to optimize the operation of heat pumps and photovoltaic systems. One study introduced a safe reinforcement learning approach for multi-energy management in smart homes [7]. Another one explores an approach of reinforcement learning for managing energy in homes, specifically operating heat pumps and PV systems [14].

Another study analyzed a combined solar thermal heat pump system's performance for heating for residential buildings [15]. The effective operation and substantial reduction in energy consumption of a well-designed solar thermal heat pump heating system, particularly in comparison to conventional heating systems utilized in cold climate structures, constitute the key findings of this study.

1.5. Knowledge Gap and Thesis Objective

In line with scientific principles, this project seeks to boost knowledge and address specific gaps. This section outlines the identified gaps and the overall goals of the thesis.

1.5.1. Knowledge Gap

The primary knowledge gap addressed by this thesis involves adding new features and expanding the application scope of the PVMD Toolbox. As discussed in the subsection 1.1.1, the toolbox is currently limited to analyzing and managing solar energy exclusively with PV panels. However, it lacks the capability to explore how the energy generated by these panels can be utilized. This project seeks to fill this gap by incorporating additional technologies, such as heat pumps and batteries. By integrating the AC output of the toolbox, the aim is to develop a comprehensive solution for residential houses.

This thesis project also endeavors to address another knowledge gap, specifically by examining the multi functional capabilities of heat pumps. It seeks to investigate how the integration of heat pumps, catering to space heating, cooling, and domestic hot water needs simultaneously, influences the overall electricity consumption profile of a household. This holistic approach aims to provide a more comprehensive understanding of the impact of heat pump applications on residential energy consumption.

Moreover, this thesis aims to explore the feasibility of integrating PV, heat pump, battery, and the grid from both technical and financial perspectives. By assessing key parameters, the study aims to determine whether such an integrated system enhances grid independence and presents a compelling investment opportunity for homeowners.

Finally, this thesis is intended to examine how the performance and cost of the combined energy system comprising PV, heat pump and battery are influenced by different weather and climate conditions in various global locations. Insights into the impact, viability, and effectiveness of these systems will be gained by observing them across different regions.

1.5.2. Thesis Objective

The idea that brought this thesis project was based on the aim of extending the usage area of the PVMD toolbox. With that purpose, the main goal of this thesis is defined as:

Designing and optimizing the energy systems of residential buildings in various cities with PV, heat pump and battery storage technologies by adding new features to the PVMD Toolbox.

To achieve this, the following sub-goals are listed as:

Sub-goal 1: Integrating a heat pump model in PVMD Toolbox

The space heating, space cooling, and domestic hot water functions need to be modeled. With this model, the demands for each purpose should be considered, and the electricity consumption for them should be calculated.

Sub-goal 2: Integrating a battery model and building the integration of each component in PVMD Toolbox.

A model to reflect the battery performance is essential, and an additional model that integrates PV panels, the heat pump, and the battery with grid actions should be developed to comprehensively represent the overall system.

Sub-goal 3: Optimizing the energy systems by considering technical and economical aspects for different locations using the PVMD Toolbox.

After developing the complete model, diverse locations should be selected to introduce variety in terms of climate and weather conditions, enhancing the depth of the study. Subsequently, economic and technical criteria should be assessed by varying the system size to identify trends and achieve optimal sizing for each location.

1.6. Thesis Outline

This thesis comprises five chapters. In Chapter 2, modeling approaches and the specific model for the heat pump are detailed, covering the calculation of demand and resulting electricity consumption for each function of the heat pump. Chapter 3 outlines the modeling approach for the battery, including integration with the overall system, the grid, and the existing household boiler. Moving on to Chapter 4, the selection process for locations is explained, along with the analysis of technical and economic parameters for the system and the methodology for achieving optimal sizing in each location. Finally, Chapter 5 provides a summary of the main research findings and offers recommendations for future studies.

2

Heat Pump Model

This chapter aims to reach the Sub-goal 1 which is 'Integrating a heat pump model in PVMD Toolbox' defined in the subsection 1.5.2.Therefore, the chapter provides an in-depth explanation of the heat pump models. Initially, various modeling approaches for the heat pumps will be discussed, along with an explanation of the selected approach for our model. Later in the chapter, the chosen models from the literature will be presented, along with detailed explanations of the modifications made to it.

2.1. Different Modeling Approaches

To enable integration analysis with the energy generated by PV panels and the household's heating demand, the selection of an efficient heat pump model is required. Therefore, a search is conducted for heat pump models available in the literature.

As the initial step, specific criteria for the desired model are established. Since subsequent analyses are intended to be carried out hourly throughout the year, the chosen heat pump model should operate on the same time scale. Additionally, the models should be capable of accommodating both space heating and domestic hot water heating for the heating mood, and space cooling for the cooling mood as this aligns with the thesis objective. Another desirable feature for the model is its ability to cater to various types of heat pumps, facilitating comparisons in between them. Moreover, the model should be modelled only by using Matlab, since it will be an extension to the PVMD toolbox that is written in Matlab.

Models for heat pumps can be categorized into two primary groups, each adopting distinct approaches in the literature [27]. The primary distinctions between these two approaches lie in the data requirements and their intended applications.

Firstly, there are "equation-fit models," which treat the heat pump as a black box and simulate its behavior through correlations using coefficients obtained from manufacturer data. Equation-fit models are more straightforward, as they rely solely on performance data typically supplied by the manufacturer for the operating conditions and the experimental data. While equation fit models provide mathematical representations of the data, the parameters in these equations may not necessarily correspond directly to physical characteristics of the heat pump. Equation fit models are commonly used in practical engineering applications for estimating heat pump performance, especially when detailed knowledge of the heat pump's internal workings is not required. They are useful for making predictions and optimizing heat pump systems based on empirical data [27].

Conversely, there are "deterministic models" that meticulously analyze each component of the system, applying principles of basic thermodynamics, energy and mass conservation equations. Deterministic models necessitate additional data for each specific heat pump components; which are evaporator,compressor, condenser and expansion valve; which result from dedicated measurement campaigns and are not readily available from manufacturers. Moreover, they require internal data, necessitating estimation through field experiments [32]. This approach proves valuable when examining and design-

ing particular heat pump components. They are essential for understanding heat pump behavior under various conditions, optimizing system performance, and designing more efficient heat pump systems [27].

The objective of this thesis is to integrate heat pump systems with PV production and battery storage for residential buildings. In this context, the focus is on tracking the energy required for heat pump operation and the heating energy to be supplied to households, treating the heat pump system as a black box model. Unlike an examination of the performance of specific heat pump components like the evaporator and compressor, which would necessitate a deterministic approach, the primary goal is the holistic evaluation of system integration. Additionally, the model to be developed should be exclusively coded using Matlab without the utilization of Simulink, as modeling each heat pump component would necessitate Simulink for simultaneous operation and extra packages to include thermodynamic properties. The aim is to maintain consistency with the existing Matlab-based framework and streamline the modeling process within the constrained timeline. Moreover, the insufficient internal data available for specific heat pump components, which would require field measurements, makes a deterministic model challenging. In light of these considerations and the study's constraints, an equation-fit modeling approach is chosen over a deterministic one.

2.2. The Chosen Models

After determining the modeling approach to build the heat pump model, two models have been chosen from the literature to represent the heating and cooling cycles, facilitating calculations of the COP and EER, respectively. The following sub-chapters will elaborate on the selected models and provide the rationale behind their choice. The functional details of the model and how they are integrated will be explain in the subsection 2.3.2.

2.2.1. COP Model

The model for calculating COP based on an existing equation-fit model in the literature by Ruhnau et al [31]. They introduce the 'When2Heat' dataset, which provides synthetic time series data for heat demand and heat pump efficiency in 16 European countries [31]. The data set covers the years from 2008 to 2018, offering data on an hourly basis. To create the data set, it combines standard gas usage profiles with temperature and wind speed data, along with population information, to compute heating demand for both space and water heating. Moreover, the data set includes COP data for different heat sources (air, ground, and groundwater) and heat distribution methods (like floor heating, radiators, and water heating). These COP values are determined using COP and heating curve information, leveraging temperature data.

The model they built to calculate the COP aligns well with this study in achieving 'Sub-goal 1.' This model facilitates the calculation of COP for three types of heat pump models throughout the year, on an hourly basis, matching the output of the PV model to which this study serves as an extension. The model enables the calculation of two heating functions, namely space heating and domestic hot water, with different fits. Additionally, it includes the two most common supply options for residential space heating: radiator supply and underfloor heating supply.

The strengths of the model can be listed as[31]:

- **Validity:** The dataset comprises historical time series data, eliminating the need for uncertain assumptions about future developments. The COP calculations are parameterized using manufacturer data and further validated through field measurements.
- **Accuracy:** The dataset accounts for variations in heat demand (both space and water heating), diverse heat sources (air, ground, and groundwater), and various heat sinks (floor heating, radiators, and water heating).
- **Comprehensiveness:** The time series cover a substantial geographical expanse, encompassing 16 EU countries with cold-temperate climates. This wide coverage is pertinent for modeling the equilibrium of the increasingly interconnected European electricity system. Moreover,

the dataset spans eleven years (2008–2018), facilitating sensitivity analyses related to different weather years.

- **Applicability:** The data are presented in a format that is highly aggregated spatially (at the national level) and finely resolved temporally (on an hourly basis), aligning with the formats commonly used in many European electricity market models.

2.2.2. EER Model

The model for calculating EER based on an existing equation-fit model in the literature by Mouzeviris and Papakostas [20]. In their work, a comprehensive examination is conducted on the EER, utilizing technical data from 430 distinct models of air-to-water heat pumps and ground-source heat pumps under specific conditions of ambient air, ground source, and water outlet temperatures from the heat pump [20]. The outcomes, presented graphically and in tables, showcase EER values in relation to the heat pumps' nominal capacity, illustrating the correlation between COP and EER with the temperature rise (ΔT) along the heat pump. Through averaging the performance values of all AWHPs or GSHPs models, polynomial regression equations are derived, providing the relationship between average EER and ΔT values.The results provided possess universal validity and are not contingent on specific local climatic conditions. Their outcomes were computed based on prescribed conditions of ambient air, ground source, and water outlet temperatures, as outlined in the European Standard EN14511-3:2008 [20].

The models constructed in this study align effectively with the attainment of 'Sub-goal 1' from the cooling perspective. Similar to the COP performance model, this EER model facilitates hourly calculations consistent with the overall model. Hence, it is selected to represent the cooling function of the heat pump.

2.3. Detailed Model Explanation

In this section, a detailed explanation of the model will be provided. Firstly, the relationship between COP, heating demand, EER, cooling demand and power requirements will be expounded upon. Subsequently, the methodology for obtaining heating and cooling demand data will be discussed. Following that, COP and EER calculation and the models' characteristics will be explained. Additionally, a thorough discussion of input variables will be undertaken, covering air, water, and ground sources, as well as sink-side components, including radiators, underfloor heating, and hot water systems.

In Figure 2.1, an overview of the model can be seen with a flowchart including the inputs get into the model, primary outputs that are got from the models and the final output received from the heat pump model built.

COP, EER and Power Relation

As mentioned in section 1.2, COP and EER stand out as a central characteristic of heat pumps. Understanding the significance of COP and EER is essential for our model. It represents the ratio of heat output provided by the heat pump to the input power it consumes. By employing our model to calculate COP and EER for various heat pump types and taking into account the heating and cooling demands of the household, we can accurately determine the power requirements of the heat pump. The relation can be seen in the following equation:

$$COP = \frac{HeatSupplied}{Power} = \frac{HeatingDemand}{Power} \tag{2.1}$$

$$Power_{heating} = \frac{HeatDemand}{COP} \tag{2.2}$$

$$EER = \frac{HeatExtracted}{Power} = \frac{CoolingDemand}{Power} \tag{2.3}$$

$$Power_{cooling} = \frac{CoolingDemand}{EER} \tag{2.4}$$

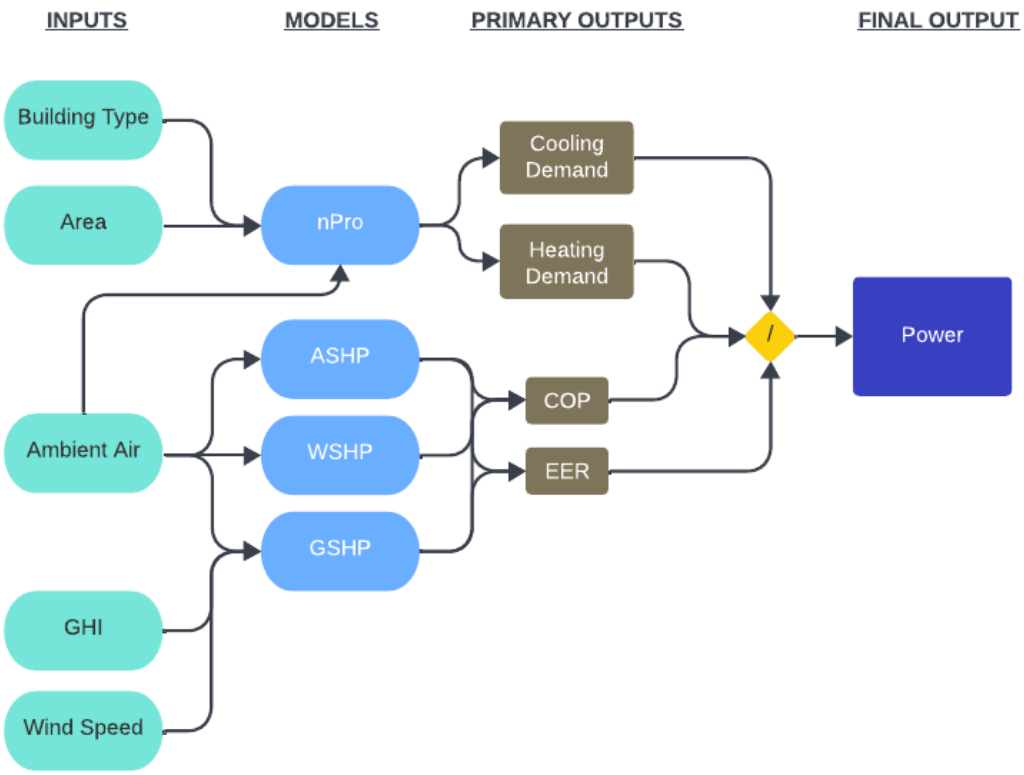

Figure 2.1: Overview of the heat pump model.

From the equations presented above, we can determine the power required for heat pump operation by calculating their respective COP and EER values.

2.3.1. Heating & Cooling Demand and NPro

Heating and cooling demand play a pivotal role in our heat pump model, as it serves as a crucial input for calculating the heat pump's power requirements. Household's heating demand can be categorized into two main components: 'Space Heating Demand' and 'Domestic Hot Water (DHW) Demand.', whereas cooling demand refers only 'Space Cooling Demand'.

Space heating demand refers to the heat needed to warm the indoor air of the house. In the northern hemisphere, this demand typically peaks during winter and decreases substantially or becomes negligible during the summer. Consequently, the external conditions affecting the house, including weather and climate, exert a significant influence on space heating demand. As a result, space heating demand exhibits a seasonal variation.

Conversely, space cooling demand involves the need to cool indoor air, and in the northern hemisphere, this demand usually peaks during the summer and diminishes significantly or becomes negligible in winter. External factors, such as weather and climate, play a crucial role in space cooling demand, resulting in a distinct seasonal variation.

Furthermore, the insulation level of the house has a substantial impact on both space heating and cooling demand. A well-insulated house, equipped with features such as double-glazed windows, HR++ glass, wall, and floor insulation, experiences reduced heat loss to the surroundings during winter and minimizes heat gain during summer. Consequently, it exhibits lower space heating demand in winter and lower space cooling demand in summer.

Domestic Hot Water (DHW) demand pertains to the energy needed to heat the water used in household

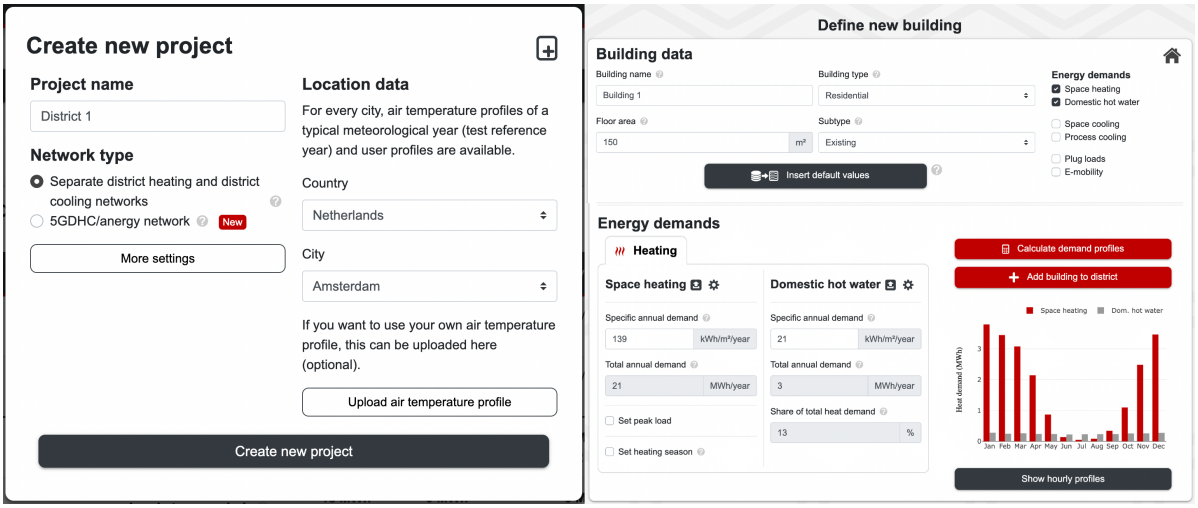

Figure 2.2: nPro interface for the heating demand.

sinks. Unlike space heating demand, DHW demand remains relatively stable throughout the seasons and is less influenced by the insulation level of the house. This demand is directly linked to the number of individuals residing in the household, as the heated water is used for various purposes such as showers and dishwashing.

To incorporate heating and cooling demand into the model, the nPro tool is utilized to obtain the necessary inputs for both space heating,cooling and DHW. nPro emerged from years of experience in district planning. While existing energy system planning tools rely on complex calculations and are primarily intended for experts with extensive experience or involvement in their development, nPro was designed specifically for the early stages of district energy planning. Its aim is to expedite and standardize the planning and quoting process for district projects. What sets nPro apart is its integration of established calculation techniques into a user-friendly interface, emphasizing usability. Notably, nPro specializes in the calculation and design of district heating and cooling networks, as well as 5GDHC (anergy) networks, employing innovative mathematical optimization methods. [23]

nPro calculates both space heating and cooling using the simplified relation between the outside air temperature and inside air temperature. The energy required for heating and cooling homes is influenced by the weather. In extremely cold winters, more energy is consumed for heating compared to milder winters, while in hot summers, more energy is needed for cooling. To determine the average annual energy requirement, the measured data can be adjusted based on weather conditions. In the nPro system, hourly annual ambient air temperatures is the input. To ensure consistency with the PVMD Toolbox, data from Meteonorm is utilized. nPro also considers the building type for calculations. The nPro tool includes heat demand and peak heating load data specific to various building types across the globe. [25]

The nPro tool offers estimated domestic hot water needs tailored to various building types for reference purposes. This includes data from statistical surveys and national standards found in the literature. [24]

To obtain heating and cooling demand data, an academic-purpose account is created. In Figure 2.2, the tool's interface is displayed. Firstly, the country and city are specified within the tool. Following that, the ambient air temperature can be manually added. The subsequent step involves the selection of the house's area. Afterward, the building type and building subtype are chosen. For the heat pump model, space heating, domestic hot water and space cooling demands are selected. By inserting values, the data can be observed. The data comprises 8760 values, representing hourly data for an entire year.

2.3.2. COP Calculations

The following COP calculations are adapted from the model by Ruhnau et al. [31]. In the model, the COP time series are derived from quadratic COP curves, which consider the temperature difference between the heat source and heat sink as an input parameter. These curves are parameterized using manufacturer data and are categorized into three heat pump types: air-source heat pumps (ASHP), ground-source heat pumps (GSHP), and groundwater-source heat pumps (WSHP).

Heat source temperature time series for air and soil are extracted from the ERA-Interim archive, while a constant water temperature is assumed by Ruhnau et al. [31]. However, to be consistent with PV calculations in my model, Meteronorm inputs are used for the following calculations, and variable water temperature is adjusted. Heat sink temperature time series are computed using literature-based heating curves for floor heating and radiators, with the hot water supply temperature held constant.

Under the assumption of uniform adoption of different heat pump technologies across various locations within each country and across different building types, the spatial COP profiles are aggregated at the national level in accordance with heat demand. Finally, the time series are adjusted based on field measurements. Because, there is a notable distinction emerge between COP time series and field measurement. The observed differences can be attributed to the assumption that manufacturer data used for COP curve regression were obtained under ideal operating conditions. In practical terms, ideal conditions involve steady-state operation at full load. In real-world scenarios, adjustments to heat pump operation in response to prevailing demand levels are made, introducing losses. Hence, a correction factor of 0.85 is applied to each model on an hourly basis during the calculations as defined in the model. [31]

In the following section, equation-fit models for three different types of heat pumps will be discussed. They all follow the same logic. As mentioned previously, each type of heat pump has two inputs: the source-side temperature and the sink-side temperature. In these models, ΔT is the variable that varies at each time step. In the equations, ΔT represents the following:

$$\Delta T_{h,l}^{sink,source} = T_{sink} - T_{source} \tag{2.5}$$

The models for three of the heat pumps are comprised of polynomial fits in which the temperature difference serves as the variable in the equations. The equations for all three of the heat pumps take the form of:

$$COP = C1 + C2 * \Delta T + C3 * \Delta T^2 \tag{2.6}$$

The coefficients that are used in the equations for COP for each heat pump are given in Table 2.1a and COP's behaviour to the changing temperature is shown in Figure 2.3.

Air Source Heat Pump (ASHP)

In the ASHP model, for simplicity, only on-off modulating heat pumps are considered in the regression analysis; variable-speed ASHPs are not included.

As the source-side input for the ASHP, hourly ambient air temperatures from Meteonorm are utilized. Using the equation, COP can be calculated for each hour of the year at the desired locations[31].

Ground Source Heat Pump (GSHP)

The source-side temperature data for GSHP is generated using the ground temperature equation from Meteonorm, with the ambient air temperature T_a, wind speed WS, GHI, and albedo number a as variables, as shown in the following equation[18]:

$$T_g = T_{amb} + [0.015 * (1 - a) * GHI - 0.7] * exp(-0.09WS) \tag{2.7}$$

In the manufacturer's data, the source-side temperature is referred to as brine temperature instead of ground temperature. To align with the manufacturer's data, a subtraction of 5 K is performed from the ground temperature, and it is used as the source-side temperature for the GSHP model.[31] Using the equation, COP can be calculated for each hour of the year at the desired location.

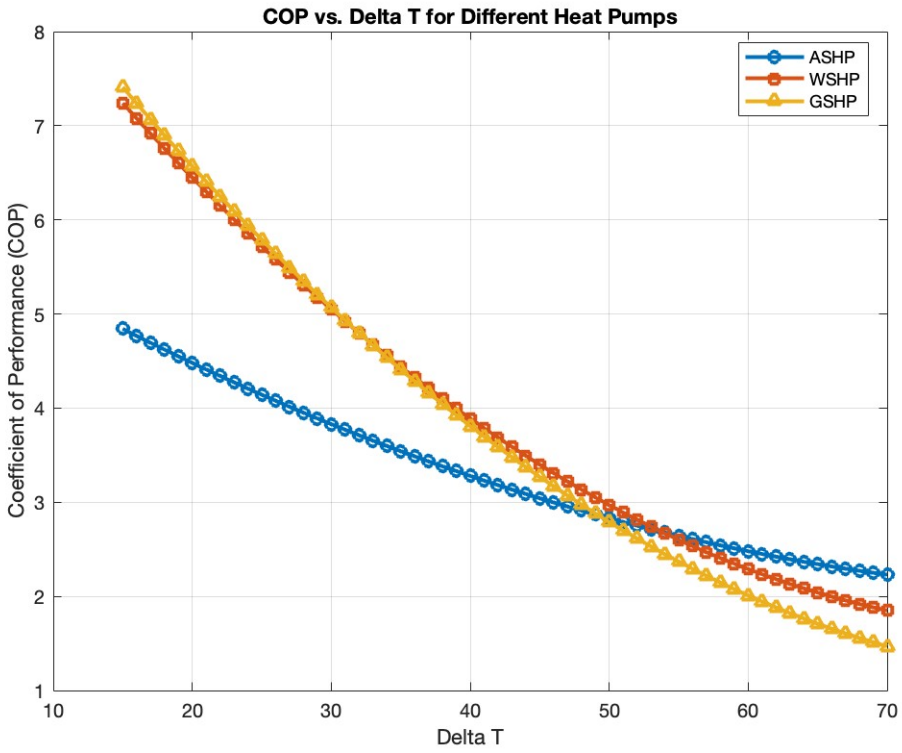

Figure 2.3: COP of different heat pumps for variying temperature difference.

Water Source Heat Pump (WSHP)

For the water source heat pump model, a fixed temperature of 10 degrees Celsius is used as the source-side temperature for simplicity.[31] However, the water side temperature varies with changes in the ambient air temperature. To account for this and improve the accuracy of the source-side temperature, an additional model is looked for specifically for the source side.

In the model, the relationship between the ambient air temperature and lake-water temperature for the water source heat pump was investigated. After fitting the data with four different models (Boltzmann, Gauss, Linear, Polynomial), the most accurate fit was obtained using the linear model.[45] The correlated version of the water temperature fit is as follows:

$$T_w = 0.74 * T_a + 4.22 \tag{2.8}$$

The prediction model for the source side as the water temperature can be used for the temperature determination in other lakes that has 4 meters depth and similar climate to Xiangtan, where the model is built for. The climate is cold-winter and hot-summer climate [45].

After getting the hourly water side temperature using the ambient air temperature, COP for the WSHP can be calculated for each hour of the year at the desired location[31].

Sink Sides

To calculate the corresponding COPs, a temperature difference is required, as mentioned in Equation 2.11. Therefore, the heat sink temperatures are computed for radiator heating, floor heating, and water heating. For space heating purposes, either radiator heating or floor heating serves as the sink side. In the case of domestic hot water (DHW) usage, water heating functions as the sink side. Consequently, the space heating and DHW demand profiles collected from nPro are associated with radiator&underfloor heating and water heating, respectively.

	Coefficients		
Heat Pumps	C1	C2	C3
ASHP	6.08	-0.09	0.0005
GSHP	10.29	-0.21	0.0012
WSHP	9.97	-0.20	0.0012

(a) Coefficients for COP Calculations

	Coefficients		
Heat Pumps	C4	C5	C6
ASHP	5.8115	-0.154	0.0014
GSHP	7.4433	-0.199	0.0015

(b) Coefficients for EER Calculations

Table 2.1: Coefficients for Heat Pump Calculations

For radiator and floor heating, the sink-side temperatures are determined using the ambient air temperature. The heating curves are derived by calculating the average of those found in the literature for the model[31], which are inversely related to ambient temperature since lower outside temperature requires higher supply temperature to give the same comfort level in the household, and they can be calculated hourly as follows:

$$T_{sink,rad} = 40 - T_{amb} \tag{2.9}$$

$$T_{sink,floor} = 30 - 0.5 * T_{amb} \tag{2.10}$$

For water heating, a constant sink temperature of 50 degrees Celsius is adopted, taking into account the German field measurements.[31] Regarding DHW, rather than modeling the water tank, only the energy demand is considered, and a fixed temperature for the water tank is selected for simplicity. This choice aligns with the model's primary focus on demand and the energy required to meet it. However, despite the data providing hourly DHW demand, an approach closer to the buffer tank method is employed, wherein the total daily demand is aggregated and supplied during the peak PV supply period at noon. This adjustment is made within the Matlab code.

2.3.3. EER Calculations

The following COP calculations are adapted from the model by Mouzeviris and Papakostas [20]. In the model, the EER time series are derived from quadratic COP curves, which consider the temperature difference between the heat source and heat sink as an input parameter. These curves are parameterized using manufacturer data and are categorized into two heat pump types: air-source heat pumps and ground-source heat pumps.

The calculation of the EER follows the same logic as COP calculations, using ΔT as the variable in the equation. However, this time the system is reversed. The inside of the house becomes the source where the heat is extracted, and the outside becomes the sink where the heat is delivered. This designates the ambient air and ground temperature as the sink side temperatures. Meteonorm data is utilized for the ambient air, while Equation 2.7 is referenced for the ground temperature, as in the COP calculations. For cooling applications, a standard source side water temperature of 10 degrees Celsius is used, as commonly adopted in the field [20].
The equations for the heat pumps to calculate EER take the form of:

$$EER = C4 + C5 * \Delta T + C6 * \Delta T^2 \tag{2.11}$$

The coefficients in the equation can be seen in Table 2.1b and the EER's behaviour to the changing temperature is shown in Figure 2.4.

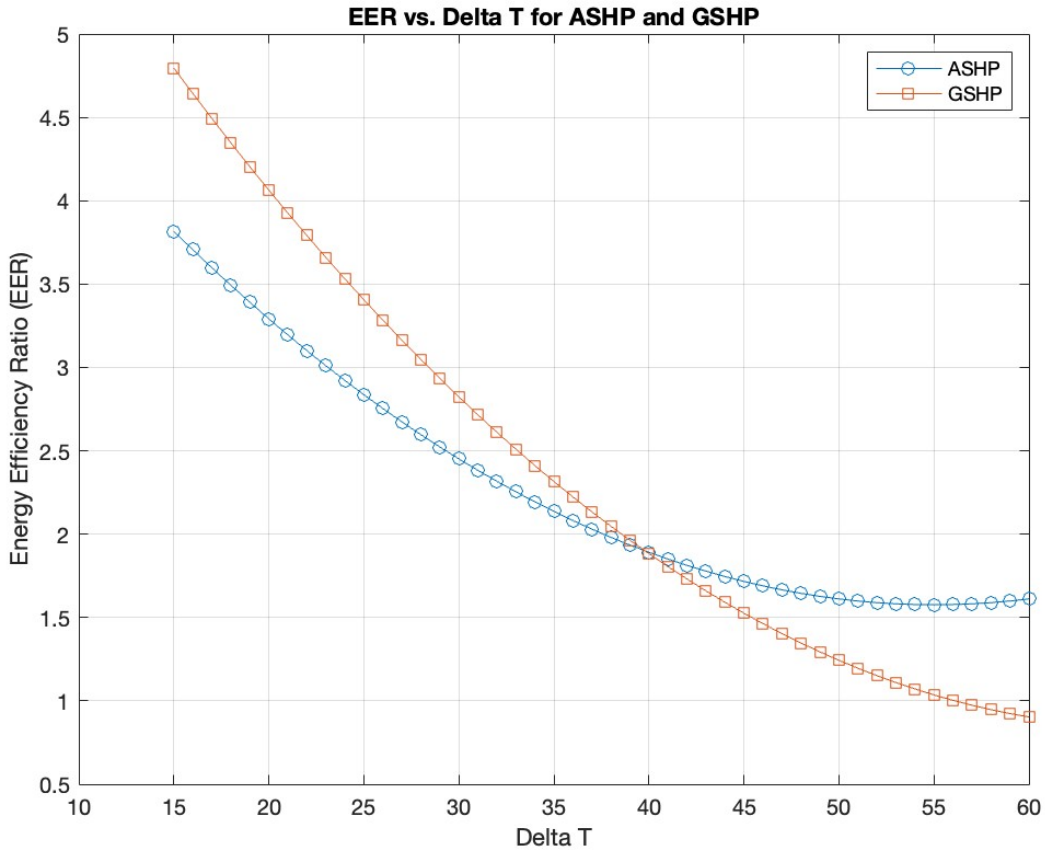

Figure 2.4: EER of different heat pumps for variying temperature difference.

2.4. Conclusion

In conclusion, this chapter has successfully addressed the primary objective outlined in Sub-goal 1 that is 'Integrating a heat pump model in PVMD Toolbox', which aimed to add the models of heat pumps for space heating, space cooling, and domestic hot water functions. The comprehensive exploration of different modeling approaches for heat pumps, including equation-fit and deterministic models, was undertaken to identify the most suitable approach for integration with the overall framework of the study.

Two specific models were chosen for COP and EER calculations, aligning with the goals of the study. Moreover, the chapter outlined the relationships between COP, EER, and power requirements, emphasizing the significance of these parameters in determining the energy efficiency of heat pump systems. The explanation of heating and cooling demand, as well as the use of the nPro tool, demonstrated the methodology employed to obtain crucial input data for the models.

The chapter successfully fulfilled the Sub-goal 1 and laid the foundation for the subsequent integration of heat pump systems with PV production and battery storage for residential buildings.

3

Battery Model and Integration

This chapter aims to address the defined 'Sub-goal 2' that is 'Integrating a battery model and building the integration of each component in PVMD Toolbox' in subsection 1.5.2. It starts by examining various battery modeling approaches found in the literature. Subsequently, the chosen approach will be introduced and justified. Following this, the inputs for the battery model and the model's key features will be elaborated upon. In the integration subchapter, each component of the entire system will be examined, detailing their utilization as inputs for the model. The chapter then provides a comprehensive explanation of how the model operates, accompanied by an illustrative example integration scenario.

3.1. Battery Modelling

It is crucial to model the battery in order to gain a thorough understanding of battery performance, including accurate insights into battery efficiency during charging and discharging, the state of power, the state of charge, and battery health. Having a model that can provide these insights is necessary for a comprehensive analysis of the techno-economic behavior of the system.

In the literature, batteries can be modeled using various approaches, which vary in terms of complexity and accuracy, as well as their intended purposes for different applications. These different modeling approaches can be categorized into three main groups: electrochemical, equivalent electrical circuit, and mathematical models[35].

The first modeling strategy, electrochemical modeling, has the highest accuracy ranking since it represents the physicochemical properties of the battery. It is based on extensive laboratory measurements.Electrochemical models concentrate on investigating the chemical reactions occurring within electrodes and electrolytes. Mathematical tools such as Non-Linear Differential Equations, Partial Differential Equations, and ODE are employed. Unless these equation systems are streamlined, the computational resources required for running these models can be extensive. Typically, the computers utilized should have capabilities for Computational Fluid Dynamics (CFD) [29]. However, due to the extremely detailed nature of the model, it exhibits very high computational complexity and cost. Therefore, this modeling approach may not be suitable for power and dynamic system simulations[35].

Electrical models are represented by equivalent circuits. An electrical model, focusing on voltages, currents, resistances, and capacitances, characterizes the electrical behavior of a battery. With consideration for system parameters that vary with temperature and state-of-charge (SOC), the resulting equations, derived from the concept of passive electrical systems, form a low-level structure of ordinary differential equations typically exhibiting non-linearity [29]. These models have lower accuracy and capture less of the physicochemical aspects compared to electrochemical modeling. However, they are considered a compromise between mathematical models and electrochemical models, as they describe the electrical performance of the battery cell in terms of voltage and current[35].

A mathematical model is the simplest type of battery model as it reflects the battery's status based

Table 3.1: Parameters of performance for the three different battery technologies.

		Battery Technology		
Parameters	**Unit**	**PbA**	**LFP**	**NMC**
Round-trip efficiency	%	85	98	95
Usable SOC	%	50-100	5-95	5-95
Indicator of calendric life time	years	10	15	13

on the energy balance mechanism. It assumes that the battery charges and discharges at a constant voltage. Consequently, it does not capture the dynamic behavior of the battery during charging and discharging processes. Mathematical models are primarily derived from battery datasheets and empirical equations. Despite their reduced accuracy and lack of physicochemical detail, they are the most commonly used modeling approach for simulating batteries in renewable energy systems[35].

Considering the features and potential application fields of each modeling approach, the choice for integration is the mathematical model. Several reasons underpin this decision. The electrochemical approach is excluded due to its complexity. While the equivalent circuit appears to strike a balance between complexity and practicality, there is insufficient data available to track voltage and current for each time step. Furthermore, this level of detail is unnecessary given the study's objectives.

When comparing electrical circuit and mathematical modeling for design scenarios, differences in battery sizing to achieve the same self-sufficiency ratio become apparent. Mathematical models tend to suggest larger sizes, with their accuracy fluctuating in the range of 5-20% [35]. However, the primary focus of the study is to explore the integration of batteries with the rest of the system, understanding their mutual influence and impact on the final system cost as a trend. The main emphasis lies in integration while considering the energy balance of the system, aligning with the application area of mathematical modeling. Moreover, when contemplating the integration of the rest of the system, which includes PV panels and a heat pump, the focus on energy balance and the utilization of an hourly battery model further supports the choice of the mathematical modeling approach.

Since the mathematical model is chosen as the modeling approach to reflect the characteristics of the specific type of battery selected, it is crucial to input the necessary battery properties into the built model. As mentioned in section 1.3, lithium-ion battery technology is selected for its energy density and lifetime cycles. The characteristic parameters are sought from the literature, and given for different battery technologies to facilitate a comparison between them, aligning with the expert knowledge of Battery Energy Storage System (BESS) manufacturers [11]. These characteristic parameters are presented in the Table 3.1.

Since the mathematical battery modeling approach assumes the battery operates with an ideal constant voltage during the charging and discharging processes, the charging efficiency η_{ch} and discharging efficiency η_{dsch} are also considered constant, equal to the square root of battery's round-trip efficiency[35]. The round-trip efficiency $\eta_{round-trip}$ is defined as the average round trip Watt-hour retention under standard conditions, involving typical low charge and discharge rates of 0.1 C (capacity-rate) and ambient temperature (around 25 ◦C). These conditions closely align with the scenarios commonly encountered in a typical home storage system[11].

$$\eta_{ch} = \eta_{dsch} = \sqrt{\eta_{round-trip}} \tag{3.1}$$

Each battery technology has a SOC range that the battery should maintain after every charging and discharging cycle. In the model to be built, this range should be tracked for each hour. To achieve this, the coulomb counting method is employed. This method checks the SOC of the battery for each time step, considering SOC of the previous step, in addition to the amount of charging or discharging energy relative to the total capacity of the battery bank. The coulomb counting method can be expressed by the following equation, where S_1 and S_2 take on values of either 1 or 0. During charging, S_1 equals 1 and S_2 equals 0, while during discharging, it is the opposite [11].

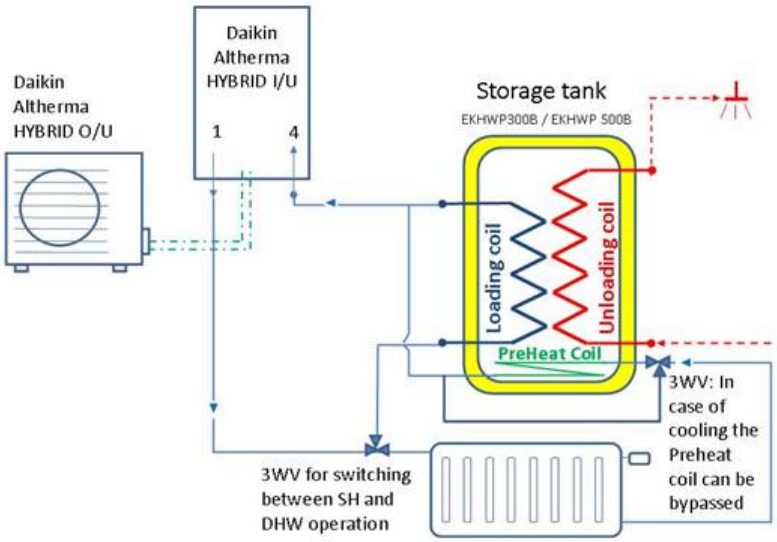

Figure 3.1: The configuration of the heat pump system.

$$SOC_{t+1} = SOC_t + S_1 * \frac{\eta_{ch} * P_{ch,t} * t_{ch,t}}{C_n} - S_2 * \frac{P_{dsch,k} * t_{dch,k}}{\eta_{dch} * C_n} \tag{3.2}$$

As seen in the equation, the amount of energy that comes to the battery $P_{ch,t}$ and the amount of energy leaves the battery $P_{dsch,t}$ during discharging is tracked and compared with the total capacity of the battery C_n to calculate the SOC for the next time step.

3.2. Integration

In this sub chapter, the modeling of integration for the analysis will be discussed. Firstly, the inclusion of each component as an input to the model is explained, covering the heat pump, PV panels, battery, and the grid. Throughout the explanation, a random scenario is presented to demonstrate the model's functionality for each component and the entire system. Afterward, the entire system is discussed, presenting its operational logic and an explanation of the system configuration.

The scenario represented in this section is randomly selected to demonstrate the functionality of the integration model.The house to be investigated is chosen as an existing 100 m^2 residential one in nPro for the location of Amsterdam, Netherlands. Details and sizes of each component will be explained within their respective subsections.

3.2.1. Heat Pump

The capacity of the heat pumps is determined based on the maximum heat supply they can provide to the sink. Since the heat pump model built is conceived as a hybrid heat pump system that works in conjunction with the existing boiler in the household, in situations where the heat pump is insufficient to meet the heating demand of the house, the boiler kicks in and covers the gap by burning natural gas, as part of its usual operation. The boiler efficiency for its performance is taken as 92% as the market average. [21]

For the demonstration scenario, air-to-water heat pump with radiator space heating, domestic hot water and cooling supply is selected and the capacity of the heat pump is set at 5 kW. Therefore, during the heating mode, the total amount of heat energy can be 5 kWh for space heating and domestic hot water

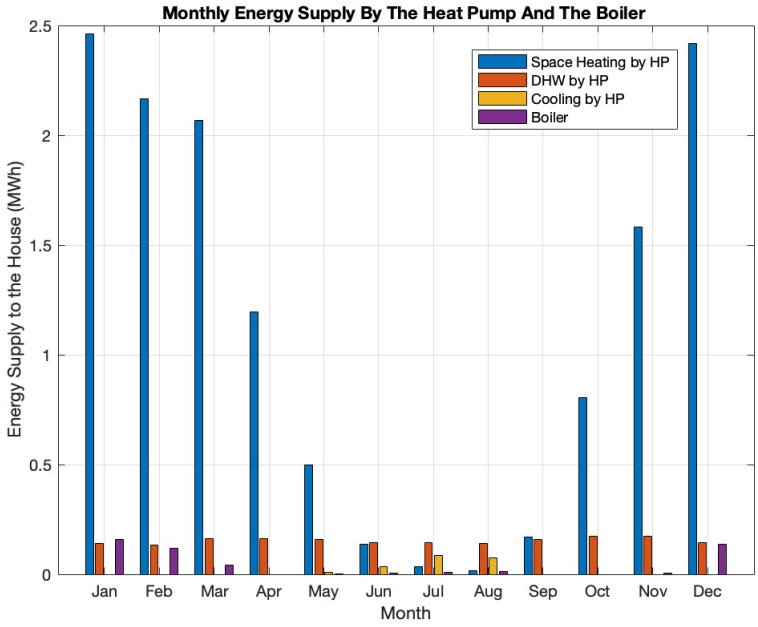

Figure 3.2: Monthly energy supply by the heat pump and the gas boiler.

combined for an hour, as the model runs hourly. In situations where the combined heat energy required exceeds this capacity, priority is given to space heating energy, and any excess energy is supplied by the existing gas boiler in the household. The schematic representation of the model can be seen in Figure 3.1.

The heat pump is configured to provide space heating energy when the ambient air temperature drops below 15 degrees Celsius and cooling energy when the ambient air temperature rises above 25 degrees Celsius, taking into account the comfort temperature inside the house. Additionally, as the heat pump cannot operate in both heating and cooling modes simultaneously, during the cooling period, cooling takes priority, and domestic hot water supply is handled by the existing gas boiler.

As seen in the Figure 3.2, space heating demand peaks out during the winter months, and boiler covers the parts where the heat pump cannot provide enough. Also, heat pump only operates in cooling mode during summer. If there is no cooling demand for the time frame, the heat pump can provide the domestic hot water demand instead.

3.2.2. Electricity Consumption

The electricity consumption of the household consists of two main components. The existing consumption is derived from the plug loads in the house and received from nPro. The other consumption comes from the operation of the heat pump. As mentioned in chapter 2, the power consumption of the heat pump is calculated using the COP for heating and EER for cooling. Therefore, the total electricity consumption to be loaded into the integration model can be expressed as follows, and can be seen in Figure 3.3

$$Electricity\ Consumption = P\ L + HP_{space\ heating} + HP_{dhw} + HP_{cooling} \tag{3.3}$$

where the total electrical consumption of the households is represented by plug loads in the house PL, the electrical consumption of the heat pump for space heating $HP_{space\ heating}$, for dhw supply HP_{dhw} and for space cooling $HP_{cooling}$.

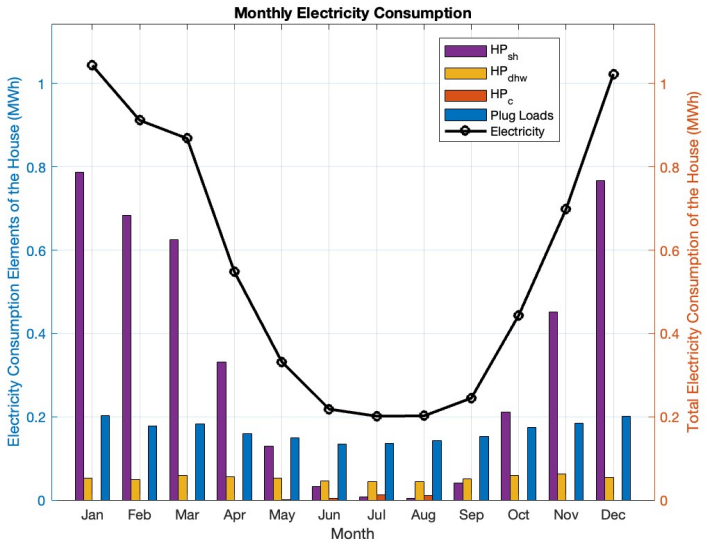

Figure 3.3: Monthly electricity consumption for the household for each application and total electricity consumption.

3.2.3. PV Panels and PV Production

The primary energy source in the integrated system is the PV production. These panels are intended to be installed atop the household, on a flat roof. In the integration model, the AC production of the panels serves as the input for the PV side.

The PV input is obtained from the PVMD Toolbox [40]. Several steps are followed to derive the ultimate AC output of the panels. It starts with modeling the cell. The toolbox uses net radiation method to simulate the optical properties. The next step is to model the module. For simplicity, periodic properties are selected, assuming that all panels have the same properties. With these assumptions, all of the panels have the same incident energy and operating temperatures. This does not reflect reality, considering the it assumes all of the panels experience the same external conditions. This method do not consider shading that the panels could experience in a residential panel placement. However, this method is chosen for its simplicity over non-periodic methods due to the additional modeling complexity it requires.

The next step is to load the weather data. For this, Meteonorm data is used. No horizon is selected. With these assumption, the panels can be thought of as if they are placed on an open field. This does not reflect reality, considering this study is conducted for residential applications. However, it is chosen for simplicity and due to the lack of data for other locations to be analyzed in the next chapter. Clear sky is selected for the spectra. For thermal modeling, the fluid dynamic model is used to detect the temperature of the panels and reflect its affect to voltage, current and power.

Later, for the electrical output, the datasheet of the PV Panel is used as input to the toolbox and can be found in appendix, and metallization losses are ignored. Finally, for the conversion output that provides the AC output of the panels, inverter selection is done, and the configuration of the panels is indicated with the number of series and parallel connections. For the example scenario, a configuration of 4 series and 4 parallel panels is selected. For the inverter type, a string inverter is chosen, considering that it is most commonly used for residential applications.

This string configuration, combines the benefits of both central inverters (simple structure) and micro-inverters (high-energy yield). Mismatch loss is minimal due to the use of MPPT at the string level, resulting in increased energy production. String architecture is commonly employed in medium-power applications (1–10 kW) for residential use, where each PV string is connected to an inverter. To address local and global Maximum Power Point (MPP) under low irradiation conditions, hybrid MPPT techniques are employed with string inverters [13].

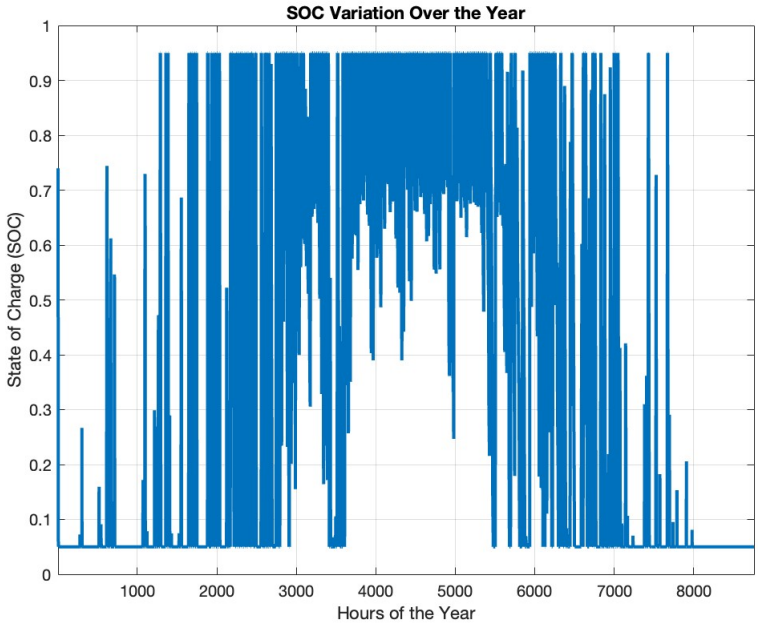

Figure 3.4: SOC variaton for the lithium-ion battery throughout the year.

3.2.4. Battery

The battery can be seen as the backup energy supply in the PV-BESS. Additionally, it provides flexibility for the renewable energy to be stored when not demanded by the household. Therefore, it compensates for the intermittence of the PV supply.

For the example scenario, the capacity of the lithium-ion battery is selected as 6200 Wh, and the properties mentioned for the lithium-ion battery in Table 3.1 are used as input for the integration model. With the battery model built within the integration model, it is possible to keep track of the amount of energy charged, discharged, total energy of the battery, and the SOC for every hour of the year.

As seen in the Figure 3.4, SOC always stays in the defined range, and fluctuates due to the charging and discharging cycles.

3.2.5. Grid and The Overall System Configuration

The overall system can be summarized as a grid-connected PV-BESS system. The system to be analyzed is designed as grid-connected instead of standalone. This choice is crucial for ensuring an uninterrupted energy supply to the house. The house can only have a reliable energy supply by being connected to the grid due to the intermittent energy supply of PV panels and the limitations of the battery system.

There are several configuration options for the PV-BESS system, depending on where the battery storage is located in the configuration. In DC-coupled configurations, the battery is connected to a battery converter, and the solar panels are connected to a PV converter. These converters are linked to a DC bus that connects all of them to the inverter, which converts direct current to alternating current for both the load and grid sides [33]. On the other hand, in AC coupling, instead of being connected to the same DC bus, the PV is connected to a separate inverter. The battery is connected to a bi-directional inverter, operating in rectifier mode when the battery is charging [33].

In the integration model, AC coupling of battery storage is chosen for several reasons. AC coupling of battery storage can provide the broadest flexibility in terms of system design and makes retrofitting existing PV installations suitable [11]. Also, considering the string inverters used for PV and the accu-

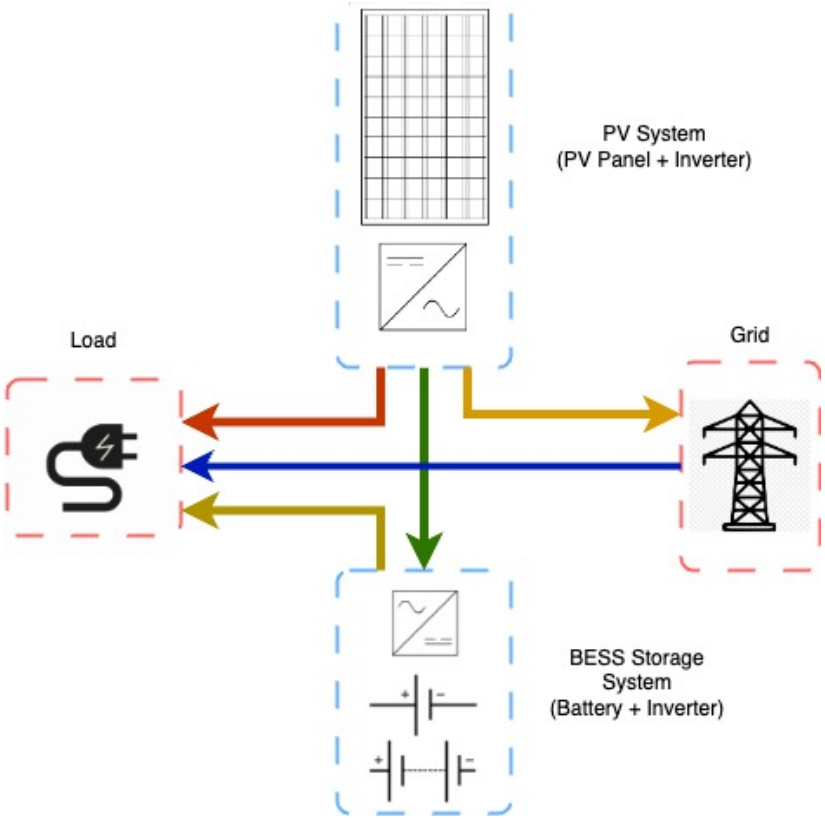

Figure 3.5: The system configuration of the grid connected PV-BESS system.

rate AC output from the toolbox, this system design does not lose any accuracy in its physical meaning with the connection of PV and battery. Moreover, even though DC system coupling topologies have their strengths and weaknesses, choosing the best technology and determining the size of the storage system is expected to follow a consistent trend when using AC coupling [11].

The configuration of the system can be seen in Figure 3.5. The arrows indicate the direction of electrical energy flows in the system. All of the transmissions are AC in the system.

The grid in the integration model serves as a backup for the other components in the system. Energy from the grid is only purchased when it is the only option and is only sold to the grid when it is neither used by the household nor stored in the battery.

The integration model is based on the energy balance, which means that at every time step, i.e., each hour of the year, the energy balance accounts for the energy produced and how it is used, or the energy to be consumed and how it is provided. The system balance can be explained with Equation 3.4.

$$E_{pv,ac} + E_{bought} + (E_{dch} * \eta_b) = E_{consumed} + E_{sold} + \frac{E_{ch}}{\eta_b} \tag{3.4}$$

To understand how the integration model works, it is important to know the control mechanism of the system. As mentioned in the previous chapters, the AC load from the PV panels, the electricity consumption for the plug loads, and the heat pump for every hour of the year, along with the battery properties and the initial SOC, are given as inputs to the model. The model runs for every hour of the year, checking the energy balance and how it can be provided for the system.

The model begins by checking if the AC production from the PV panels is more than the electricity

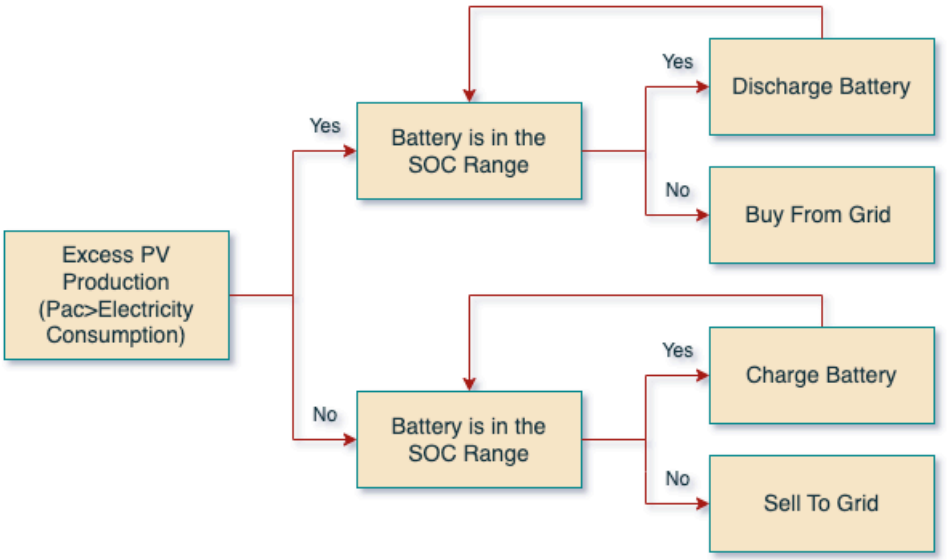

Figure 3.6: Flowchart of the integration model.

consumption of the household. If this is the case, the system first checks if the battery can be charged and prioritizes that, charging until the battery reaches its maximum capacity. After that, if there is still excess energy, this energy is sold to the grid.

In the case where the AC production from the PV panels is not enough to cover the load of the household, again, the battery performance becomes the priority. The battery discharges until the electricity demand of the house is met or it reaches its minimum capacity. In the case where the battery is not sufficient, the grid kicks in and covers the energy gap for the household. The behavior of the system can also be summarized with Figure 3.6.

To visualize the behaviour of the each component and their interaction with each other, the system behaviour is given for the first day of March and first day of August in Figure 4.11a and Figure 3.8.

March is the month when space heating demand dominates the electrical load of the house due to the heat pump operation, as depicted in Figure 3.3. Consequently, there is constant electrical consumption during the night, which increases during the day due to other appliances in the house. Since there is no solar production during the night, one can observe overlapping lines of electricity consumption and electricity purchased from the grid until daylight. The purchase of electricity from the grid decreases when the PV production begins. At midday, when solar production is at its peak, no energy needs to be bought from the grid. Moreover, excess energy can be used to charge the battery. Apart from that moment, the battery remains at its minimum charged level due to the same trend the day before and the day after. Therefore, on cold days, there is also no electricity sold to the grid.

Examining the trend on the first day of August in Figure 3.8, one can observe a completely opposite system dynamic. Firstly, there is only a small amount of electricity consumption throughout the night. Despite the absence of solar production, electricity is not purchased from the grid because the battery can supply that demand, as it is not empty. Furthermore, there is significantly more PV production. Consequently, when the battery reaches its maximum capacity, energy is also sold to the grid. On a typical summer day, one can observe that there is no need to purchase electricity from the grid for this system.

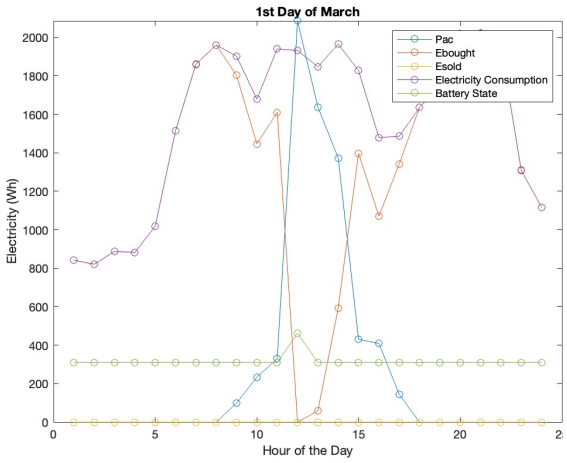

Figure 3.7: Integration model behavior during the first day of March.

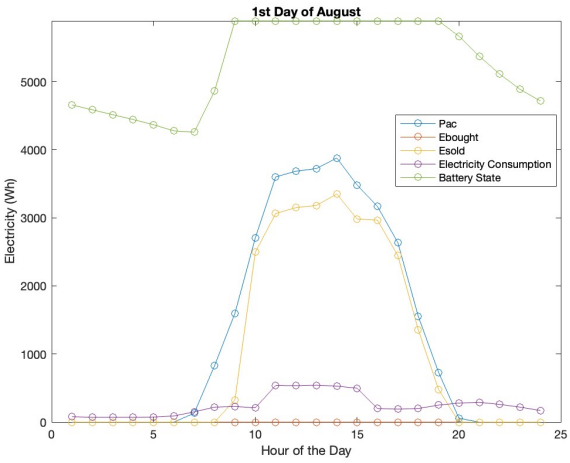

Figure 3.8: Integration model behaviour during the first day of August.

3.3. Conclusion

In conclusion, this chapter successfully achieved the goal outlined in 'Sub-goal 2' that was 'Integrating a battery model and building the integration of each component in PVMD Toolbox'. From the various modeling approaches described in the literature, a mathematical modeling approach was chosen to accurately represent the battery's performance, aligning with the objectives of the model.

Regarding the integration process, each component was systematically incorporated into the entire system. The heat pump model, previously developed in chapter 2, was integrated with household electricity consumption, taking into account its performance. Subsequently, the AC output of the PVMD toolbox was obtained and added to the model alongside the battery using AC coupling. This allowed the system to be connected to the grid, resulting in the creation of the entire integrated system.

With this model, one can analyze each component's performance throughout the year in various locations by providing the location-specific inputs. Therefore, this chapter has achieved the 'Sub-goal 2' and established the groundwork for the next objective, which involves conducting an economic and performance analysis of the system.

4

System Design and Analysis

This chapter aims to address 'Sub-goal 3' that is 'Optimizing the energy systems by considering technical and economical aspects for different locations using the PVMD Toolbox' as defined in the subsection 1.5.2. It begins with explanations of the locations where the integration model is tested and outlines the rationale behind selecting these specific locations, taking into consideration the characteristic features of the cities.

4.1. Locations

As highlighted in the conclusion of Chapter 3, the model has been developed to enable the integration of a grid-connected residential system. This system incorporates PV panels as the primary energy production source, an air-to-water heat pump for meeting cooling and heating demands while integrating the existing house boiler, and lithium-ion batteries serving as energy backup and storage for excess energy. To comprehensively understand the responses of different systems and enhance the depth of the study, it is crucial to carefully select the locations for analysis.

To introduce diversity in location selection, an initial analysis of the system is required to understand its response to different environmental impacts. Since the system relies on solar energy as its primary source, a specific examination of environmental factors affecting PV panels is necessary. These factors play a crucial role in influencing the grid interactions, including energy procurement, distribution, and the response of the energy storage system, thereby guiding the careful selection of locations for analysis.

Firstly, to create the variety in the sense of energy production from the panels, the locations are aimed to have different Equivalent Sun Hours (ESH). The energy output of a PV module is influenced by several factors, encompassing local weather conditions, seasonal fluctuations, and the specifics of module installation. To gauge and express the available solar energy, the concept of average global horizontal irradiance is utilized, measured in kilowatt-hours per square meter per day (kWh/m²/day). This metric is synonymous with the daily equivalent sun hours (ESH), providing an estimate of the solar energy received over a day. The global horizontal irradiance serves as a key indicator, reflecting variations in sunlight exposure based on factors like latitude and regional climates. As one moves towards higher latitudes, a general decrease in insolation is observed, yet regional climates introduce additional nuances to this pattern. This parameter, expressed in ESH, aids in evaluating the solar potential and optimizing the performance of PV systems under diverse geographical and climatic conditions [36].

Moreover, given that energy from PV panels is an intermittent source, the entire system and its components are influenced by this characteristic of the panels. Therefore, it is crucial to consider the variability in 'Hours of Sunlight' for the locations. 'Hours of Sunlight' refer to the duration of natural sunlight present and illuminating a specific location, directly impacting the energy production duration of PV panels.

After addressing the aspects of the energy source, it is equally crucial to consider the consumption

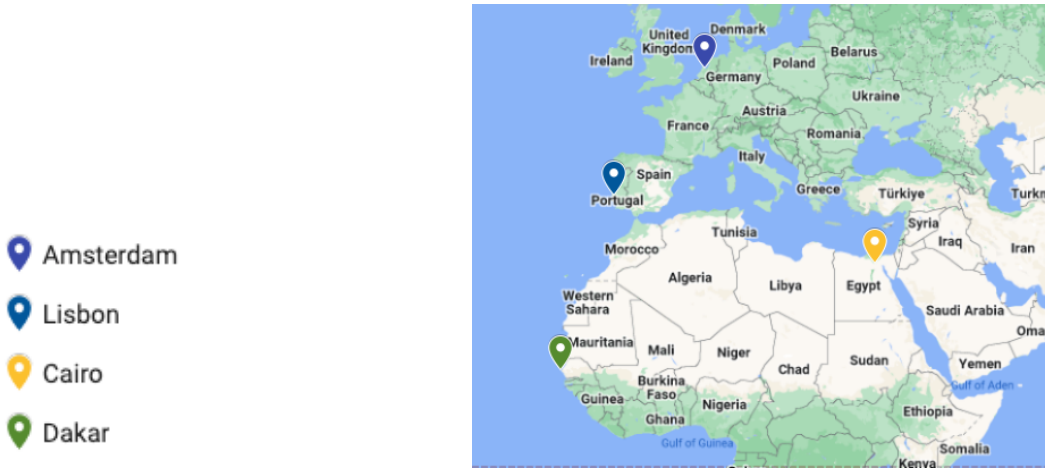

(a) Locations.

(b) Cities pinned on the map.

Figure 4.1: Cities chosen for analysis.

Table 4.1: Climate classification of the cities

Cities	Climate	Definition
Amsterdam	Cfb	Temperate, no dry season, warm summer
Lisbon	Csa	Temperate, dry summer, hot summer
Cairo	Bwh	Dry, arid desert, hot
Dakar	Bsh	Dry, semi-arid or steppe, hot

side of the integrated system. Thus, understanding the behavior of the heat pump within the system becomes imperative. The heat pump is responsible for fulfilling the heating and cooling demands of the household, and its electrical consumption is derived from these operations. As outlined in chapter 2, the model's key input is reflective of the cooling and heating demands, with the heat pump's performance being influenced by ambient air temperature. Consequently, the selected locations should exhibit diverse temperature regimes to capture variability for this purpose.

The locations are chosen considering those aspects and can be seen in the Figure 4.1. The cities are all located in the northern hemisphere, spanning different latitudes and geological positions. Consequently, they exhibit diverse climate classifications. The climate classification of the cities is provided in the Table 4.1 [2].

The ESH and Hours of Daylight information for four cities are shown in Figure 4.2. Dakar has the highest annual ESH, double that of Amsterdam, which has the lowest. Lisbon and Cairo have similar ESH values. This indicates that Dakar is expected to have the highest solar energy production, while Amsterdam has the lowest. When the monthly regimes are analyzed, the cities, except for Dakar, exhibit a similar trend, with ESH peaking around summer and reaching a minimum during winter. Additionally, the difference between the maximum and minimum values is considerable. However, Dakar maintains a more stable value throughout the year, peaking during spring and autumn. These differences can be explained by the latitudes and climates of the cities.

The Hours of Daylight for each city can be observed in Figure 4.2b. The cities exhibit a consistent trend, reaching a peak during the summer and decreasing during winter. When comparing the difference between the maximum and minimum daylight hours for each city, Amsterdam shows the most significant variation. As one moves southward, this difference diminishes, and upon reaching Dakar, it becomes evident that the contrast is minimal. Therefore, Dakar experiences a more stable duration of solar energy production throughout the year, while Amsterdam may have a higher duration of solar energy production during the summer and almost half of this production during winter. This variation

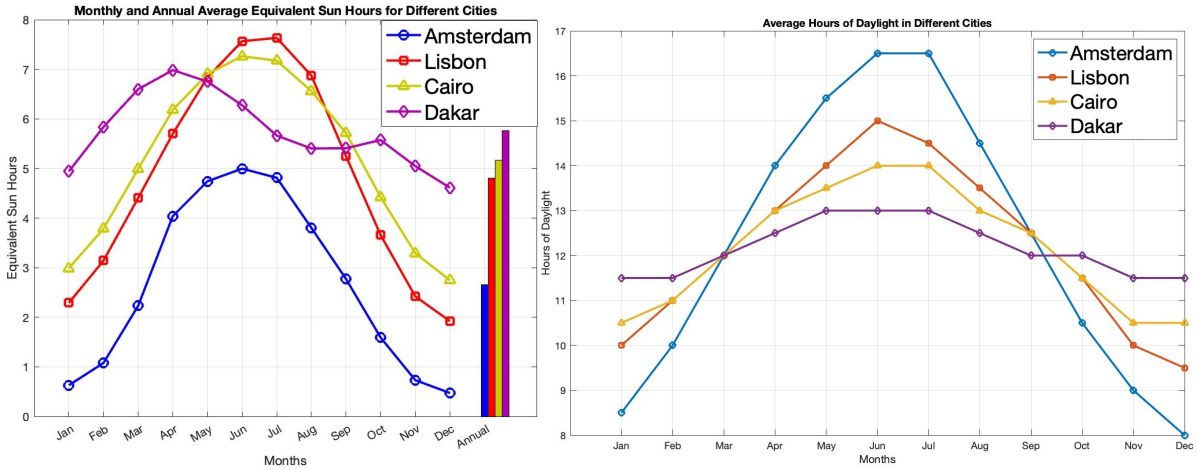

(a) ESH of the cities throughout the year and annual values.

(b) Average hours of daylight for the cities.

Figure 4.2: ESH and Hours of Daylight comparison for the cities.

can be attributed to the latitudes of the respective cities.

The monthly temperature trends of the cities are shown in Figure 4.3. Observing the monthly average values; Amsterdam, Lisbon, and Cairo follow the same trend, peaking during the summer and decreasing during the winter, with Amsterdam being the coldest and Cairo being the hottest among the three. Cairo experiences the highest temperatures during the summer, while Amsterdam reaches the lowest temperatures during winter. Upon analyzing Dakar, it exhibits a more stable trend with consistently high temperatures throughout the year and a minimal temperature difference between the maximum and minimum values.

The influence of ambient air temperature, depicted in Figure 4.3, is reflected in Figure 4.4, as it serves as the primary input for the heat pump model. A closer examination of Figure 4.4a reveals that Amsterdam exhibits the highest heating demand, peaking during the winter and diminishing during the summer, aligning with its temperature profile. In contrast, Dakar displays the lowest heating demand, specifically only in domestic hot water (DHW), with no space heating demand. Referencing its temperature profile in Figure 4.3d, it becomes evident that Dakar never experiences temperatures below 15 degrees. As mentioned in Chapter 3, space heating initiates when the outside temperature falls below 15 degrees, justifying Dakar's heating demand profile. Lisbon and Cairo present intermediate heating demand profiles between the maximum and minimum observed in the cities. Analyzing Figure 4.4b, Dakar exhibits a consistent cooling demand throughout the year, mirroring its temperature profile. Conversely, Cairo experiences peak summer cooling demands, aligning with its temperature profile.

By intentionally selecting cities with diverse values for ESH , Hours of Daylight, and temperature, it is aimed to capture a range of energy production and consumption trends. This deliberate variety in city characteristics enables in-depth analyses and facilitates a comprehensive understanding of the integrated systems in different environmental contexts.

4.2. Initial Heat Pump Size Analysis seeking Payback Period and Heating & Cooling Demand Met Ratio

Given the distinct heating and cooling demands of each city, a tailored heat pump capacity is essential for effective operation. Simply selecting the heat pump size based on maximum heating and cooling demands may lead to over sizing, rendering it economically unappealing for households. To address this challenge, the payback period and demand met ratio for both heating and cooling can be monitored by incrementally increasing the heat pump capacity, allowing the identification of an optimal size. This iterative process ensures an economically appealing solution for diverse households, striking a balance between efficiency and cost-effectiveness.

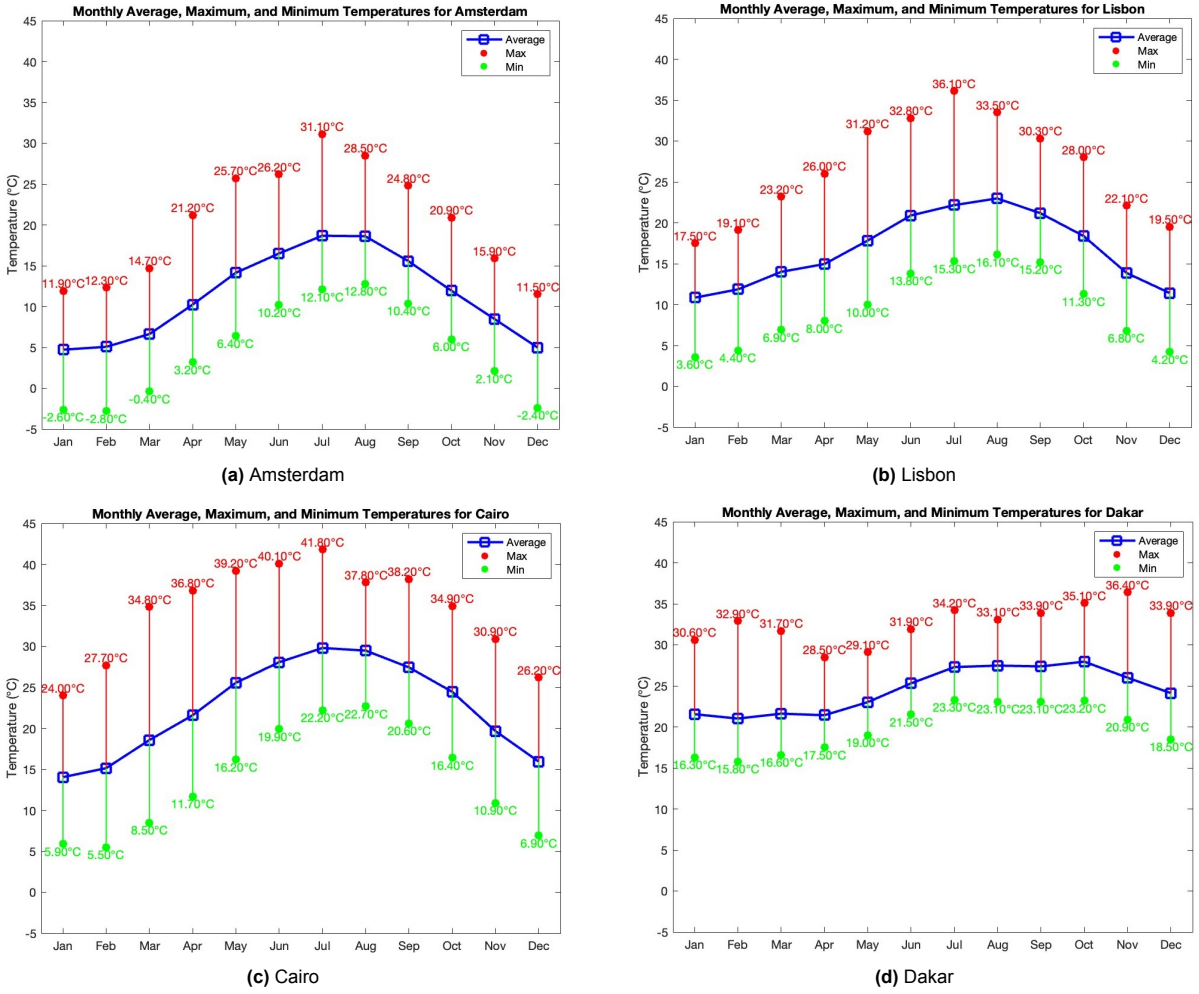

(a) Amsterdam **(b)** Lisbon

(c) Cairo **(d)** Dakar

Figure 4.3: Monthly average, maximum and minimum temperatures for the cities.

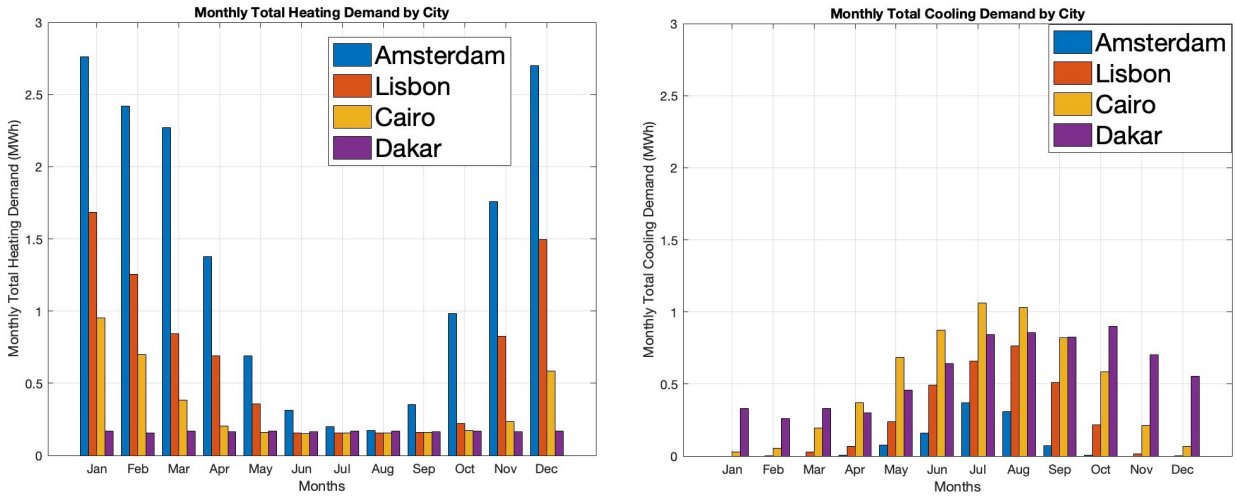

(a) Monthly Heating **(b)** Monthly Cooling

Figure 4.4: Monthly Heating and Cooling Trends.

As discussed in Chapter 3, the integrated system incorporates an existing boiler in the house that operates on natural gas. In instances where the heating demand surpasses the capacity of the heat pump, the boiler can seamlessly take over, constituting a hybrid system. Consequently, the heating demand is consistently met. The heating demand met ratio allows to quantify the proportion of this demand fulfilled by the heat pump, providing insights into its contribution to the overall heating requirements.

$$\text{Heating Ratio} = \frac{\text{Heating supplied by the heat pump}}{\text{Heating Demand}} \tag{4.1}$$

Nevertheless, when it comes to cooling, the exclusive recourse available is the heat pump, which singularly addresses the cooling demand. In this context, there is no backup plan integrated into the system for cooling purposes, makes the system rely solely on the heat pump's capacity to fulfill the cooling demand within its operational limits.

$$\text{Cooling Ratio} = \frac{\text{Cooling supplied by the heat pump}}{\text{Cooling Demand}} \tag{4.2}$$

In the absence of a heat pump, traditional boilers fulfill the heating requirements, leading to operational expenses tied to the cost of natural gas, given their reliance on this fuel. On the contrary, a heat pump functions on electricity, aligning its operational costs with fluctuations in electricity prices. Consequently, with an increase in the size of the heat pump, the electricity price emerges as the primary factor shaping operational costs. This transition highlights the potential for the heat pump to compensate for its initial investment, introducing a noteworthy factor for home owners to consider.

The heat provided by the boiler and the electrical consumption of the heat pump for heating are computed on an hourly basis using the heat pump model. The operational cost for the baseline scenario (boiler only) is derived by integrating the gas price. In contrast, for the other scenarios where the heat pump exists, the operational cost is computed by integrating both the gas price and the electricity price. The disparity in operational cost for each heat pump size is ascertained by subtracting the baseline operational cost from the corresponding operational cost.

$$\text{Payback Period} = \frac{\text{Initial investment cost for the heat pump}}{\text{Operational savings}} \tag{4.3}$$

The following assumption are made for the system and the analysis:

- At this stage of the analysis, in the integrated model, there is only heat pump, boiler and grid. Therefore, all of the electricity consumption for the heat pump operation is purchased from the grid.
- Gas price is assumed to be the average for the Europe area, at 0.1253 €/kWh [9].
- Electricity price follows a sinusoidal trend with an average of 0.25€/kWh and amplitude of 0.02€/kWh, peaking at 12:00 [21].
- The initial investment cost of the heat pump is 3000€ + 500€/kW [21].

The results of the analysis are presented in Figure 4.5. Initially, examining the trend of 'Payback Year' and identifying the corresponding heat pump sizes at the minimum points, the optimal sizes for Amsterdam, Lisbon, Cairo, and Dakar are found to be 3.5 kW, 2.5 kW, 2 kW, and 1.5 kW, respectively. This aligns with the heating demand patterns depicted in Figure 4.4a, where Amsterdam exhibits the highest capacity, and Dakar has the smallest capacity.

Even though each city reaches a minimum payback year amount, the years to reach this minimum vary significantly. The house in Amsterdam can recoup the initial investment for the heat pump in less than 2 years, whereas Dakar takes up to 40 years to compensate for the initial investment. Consequently, it is highly attractive for homeowners in Amsterdam to invest in a heat pump, while in Dakar, purchasing a heat pump may not be economically justified. This discrepancy arises from the dominance of heating

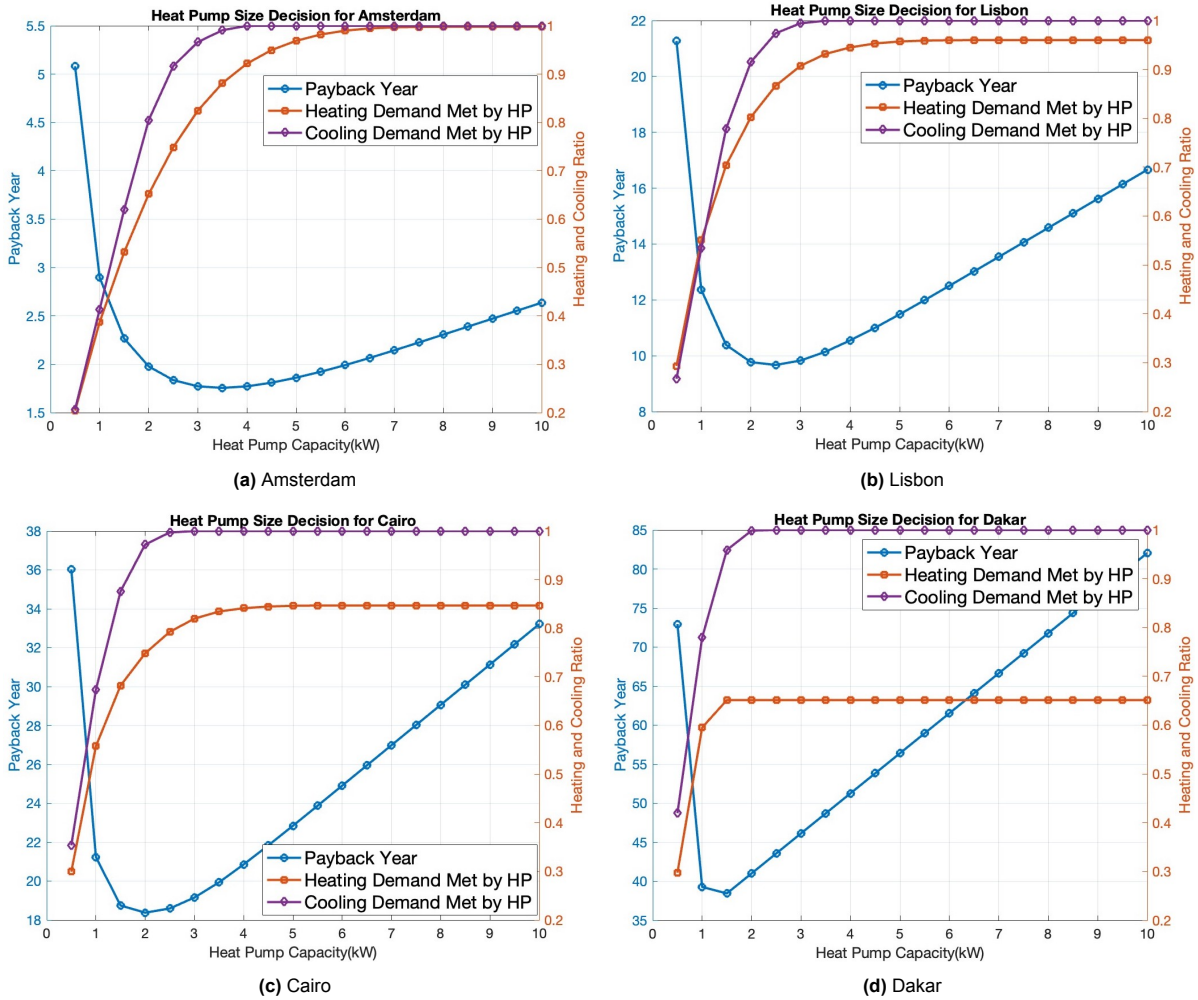

Figure 4.5: Initial heat pump size decision for the cities.

demand in Amsterdam and cooling demand in Dakar. The payback period analysis is based on the operational cost change for heating, and Dakar's heating demand is not substantial enough to benefit significantly from this cost change.

Examining Lisbon and Cairo, the operational savings can compensate for the investment cost of the heat pump within its lifetime in 10 and 18 years, respectively. Therefore, it remains an appealing investment for homeowners in those cities.

The heat pump size that results in the minimum payback year for each city aligns well with the performance prospects defined, considering the rate of meeting heating and cooling demands for each city. Cooling demand can be met for all of these cities, and the heating demand is almost fulfilled by the heat pump. The reason why it is not entirely met by the heat pump is that having a larger heat pump size is more expensive than leveraging the hybrid system and providing that small percentage with the existing boiler. Moreover, the reason why the maximum heating ratio reaches a lower point for Cairo and Dakar is that, during the period when cooling dominates, the heat pump cannot operate for its heating cycle. This limitation occurs because cooling is prioritized in the model.

The analysis reveals that the economic attractiveness of investing in a heat pump is strongly influenced by the city's unique heating and cooling demands. Cities like Amsterdam, with a higher heating demand, exhibit a rapid payback period, making the heat pump investment highly appealing for homeowners. Conversely, in cities like Dakar, where cooling demand dominates, the economic justification

Table 4.2: Initial investment costs[21].

	Fixed Cost (€)	Variable Cost
Heat pump with piping the control system	3000	500 €/kW
PV and inverter	2000	1500 €/kW
BESS	600	550 €/kWh

for a heat pump is less compelling, with a significantly longer payback period.

It is essential to note that this conclusion are drawn from an analysis based on a system dependent solely on the grid. The dynamics of these conclusions might change significantly with the integration of PV panels, battery storage, and a move towards a more self-sufficient energy model. A comprehensive approach considering solar energy and battery storage solutions could further enhance the economic feasibility of heat pump installations and reducing dependency on the grid. That initiates the next part of the analysis, where the integrated system is performed with PV panels, lithium-ion batteries and ASHP.

4.3. Integrated System Analysis with Net Present Cost Calculation

The integration model developed in Chapter 3 allows for a comprehensive overview of all activities within the system. It provides insights into the electricity consumption of the household, the contribution of PV panels to meet this demand, the grid's involvement, and the role of the battery in managing electricity exchanges throughout each hour of the year.

Considering that the system's performance is assessed over an entire year, the next step involves an economic evaluation to analyze it from the homeowner's perspective. This economic analysis will provide valuable insights into the financial aspects of the integrated system, offering a holistic viewpoint for assessment.

To determine the overall cost of the system throughout its lifetime, the Net Present Cost (NPC) can be computed. NPC provides the present value of the system, taking into account the initial investment costs of the system components and the net annual costs, which encompass expenses like electricity purchases, natural gas costs, maintenance, and insurance. The calculation involves discounting these values to their present worth, considering the rate of return. The NPC can be calculated as follows [21]:

$$NPC = I_{pv} + I_{hp} + I_{bt} + \sum_{n=1}^{20} \frac{C_n}{(1+d)^n} \tag{4.4}$$

$$C_n = C_{boiler}(1+e_{ng})^n + C_{ele}(1+e_{ele})^n + (M+Ins)(I_{hp}+I_{pv})(1+g)^n \tag{4.5}$$

where I_{pv}, I_{hp}, I_{bt} represent the initial investment costs of PV panels, heat pump and battery; C_{boiler} shows the annual cost of natural gas used in the system and C_{ele} the net annual electricity cost.

The same natural gas price and the electricity tariff trends for both purchased and sold electricity with the grid are applied to the NPC calculations, in line with the trends discussed in section 4.2. The details of the initial investment costs and economic parameters in the equations can be found in Table 4.2 and Table 4.3.

The calculations are conducted over a span of twenty years, aligning with the average lifespan of PV panels and the heat pump. As highlighted in Chapter 3, the battery comes with a lifetime of fifteen years. Consequently, the initial cost of the battery must be factored into the calculations for the fifteenth year. Given that the system assessment spans twenty years, the undepreciated capital cost in year twenty for the battery is subtracted, assuming straight-line depreciation and a €0 salvage value [17]. Therefore, the following term is incorporated into the NPC calculations.

Table 4.3: Economic parameters[21].

Symbol	Description	Value
d	discount rate	0.03
e_{boiler}	inflation rate of natural gas	0.03
e_{ele}	inflation rate of electricity	0.02
g	general inflation rate	0.03
M	initial cost fraction for maintenance	0.01
Ins	initial cost fraction for insurance	0.02

$$\frac{I_{bt}}{(1+d)^{15}} - \frac{I_{bt}\frac{2}{3}}{(1+d)^{20}} \tag{4.6}$$

The NPC calculations are conducted for each city with various system size configurations. To maintain a systematic approach, the AC PV outputs for each city are gathered from the PVMD toolbox for five distinct PV sizes: 1.08 kWp, 2.16 kWp, 3.24 kWp, 4.32 kWp, and 5.4 kWp. Subsequently, for each PV size, the battery size and heat pump size are concurrently increased to explore every conceivable combination. Following this, the heat pump is held constant while PV and battery sizes are changed simultaneously. The objective for each city is to identify the system size combination that results in the lowest NPC.

While performing the NPC calculations, it is important to check two parameters to have a better insight about the final combination. Self-Consumption Rate (SCR) that is characterized by the quantity of locally generated and consumed electricity relative to the total local generation(PV panels). Self-Sufficiency Rate (SSR) that gauges the quantity of consumption met by local generation (PV panels and battery) relative to the total consumption [5]. This metric assesses user autonomy from the grid. They can be calculated with the followings for the annual performance of the system:

$$SCR = \frac{E_{pv,ac} - E_{sold}}{E_{pv}} \tag{4.7}$$

$$SSR = \frac{E_{load} - E_{bought}}{E_{consumed}} \tag{4.8}$$

Before conducting the NPC calculations for each city with different system sizes, to provide better insight into the upcoming results, the operational cost of the systems without any PV, battery, and heat pump is calculated. The expenses include the purchase of electricity from the grid and the consumption of natural gas by the boiler. After that, the present value of the total operational cost during twenty years are calculated to give a base for the integrated systems. The values can be found in Figure 4.6 for each city. However, it is important to note that, for this system, cooling demand is not met at all. As mentioned before, there is no alternative for cooling other than a heat pump. Therefore, cooling expenses are not included in the overall costs for this system. When comparing the NPC with integrated systems for cooling demand dominant cities, this factor should be taken into consideration.

The NPC calculations are conducted for each city. Initially, the PV size is held constant for five different sizes, while the battery and heat pump sizes are simultaneously adjusted. Subsequently, the heat pump size is kept constant for five different sizes, and PV and battery sizes are changed simultaneously. The results are presented in Figure 4.7 , Figure 4.8 and Table 4.4 indicating the minimum NPC size combination for each city with corresponding SCR and SSR.

Looking at Amsterdam in Figure 4.7a and Figure 4.8a together, the minimum NPC is achieved by solely incorporating the heat pump component into the base system. The combined operation introduced by PV and battery is not financially advantageous for Amsterdam. The city is primarily characterized by heating demand, and the household's electrical consumption is mainly driven by the heat pump's heating operation. However, PV production occurs during the day, with a peak in the summer, while the

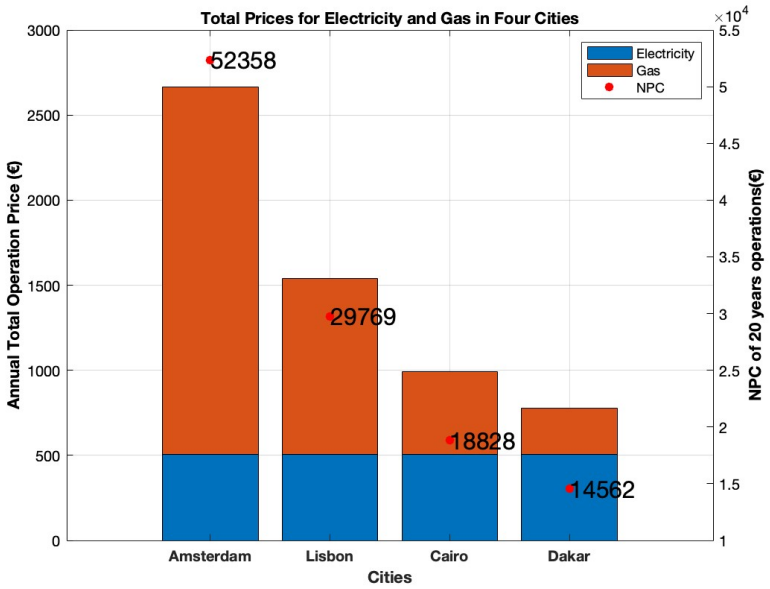

Figure 4.6: Annual operational costs and NPC for 20 years for the no component system.

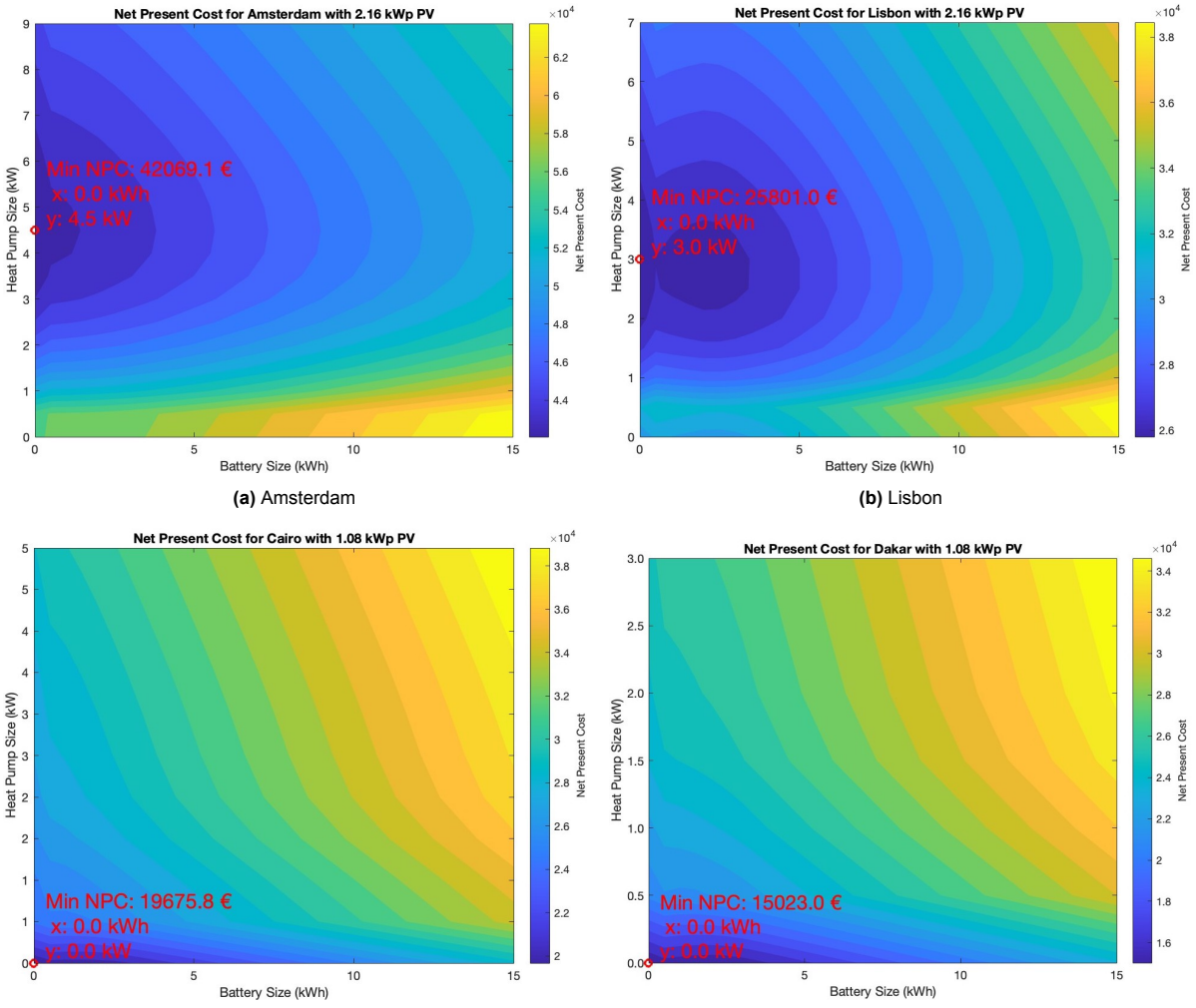

(a) Amsterdam **(b)** Lisbon

(c) Cairo **(d)** Dakar

Figure 4.7: Minimum NPC configuration for each city with fixed PV-changing battery & heat pump size.

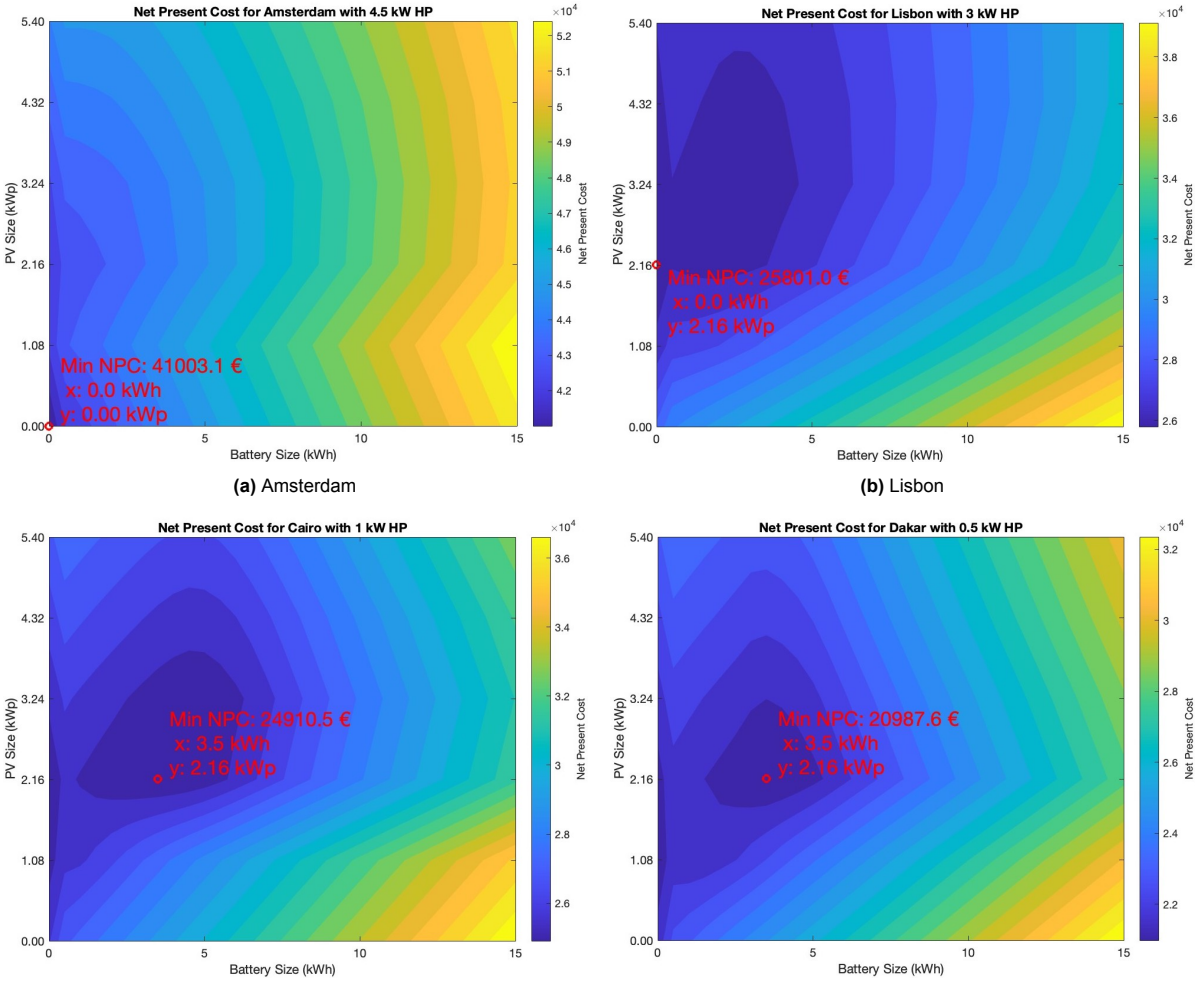

(a) Amsterdam **(b)** Lisbon

(c) Cairo **(d)** Dakar

Figure 4.8: Minimum NPC configuration for each city with fixed hp-changing battery & PV size.

Table 4.4: Results of the system configurations.

	PV(kWp)	BSSS(kWh)	HP(kW)	NPC(€)	SCR	SSR
Amsterdam	2.16	0	4.5	42069	0.64	0.20
	0	0	4.5	41003	-	-
Lisbon	2.16	0	3	25801	0.49	0.45
Cairo	1.08	0	0	19675	0.57	0.44
	2.16	3.5	1	24910	0.82	0.75
Dakar	1.08	0	0	15023	0.55	0.47
	2.16	3.5	0.5	20987	0.72	0.89

heating demand is most significant during winter nights. Consequently, when PV production is at its highest, the household's electrical load is at its lowest. Examining Table 4.4 for the initial size combination for Amsterdam, the low SSR indicates that the majority of the electrical load is supplied by the grid. Nonetheless, the addition of the heat pump contributes positively to the system's financial viability. Comparing the NPCs with the values in Figure 4.6, having the heat pump makes the system significantly more appealing for households financially for Amsterdam.

When examining Lisbon in Figure 4.7b and Figure 4.8b, it is evident that a system size combination resulting in the minimum NPC can be identified. Comparing Lisbon with Amsterdam, it becomes apparent that incorporating PV panels brings financial benefits to the system. In the case of Lisbon, despite the additional initial investment costs for a 2.16 kWp PV panel and a 3 kW heat pump, along with associated insurance and maintenance costs over 20 years, the NPC of the system is lower than the base scenario calculated in Figure 4.6. Lisbon experiences milder winters compared to Amsterdam, leading to lower heating demands and increased PV production because of its location. Consequently, the city exhibits a more balanced demand and electricity supply for households. However, the battery storage system has not yet become financially profitable with the specified prices used in the calculations.

Looking at Cairo and Dakar, a similar trend is observed in Figure 4.8 and Figure 4.7. Checking Figure 4.7, it's evident that having heat pumps is never financially profitable for those cities. Heating is not the dominant demand factor for these cities, and the financial benefit of the heat pump mostly comes from the switch from using natural gas to electricity, as mentioned in section 4.2. However, if cooling were included in the base scenario using air conditioning, the benefit would be more apparent with the heat pump, as using air conditioning increases the electricity bill by 42% during its operational seasons.

Moreover, having 1.08 kWp PV panels does not bring as much financial profit as in Lisbon, as seen from the fact that the NPC with PV panels is slightly higher than the base scenarios for those cities. The reason for this lies in the electricity tariffs defined in the calculations. Checking the SCR and SSR for those cities in Table 4.4, half of the electricity is bought from the grid, and half of the energy produced by the panels is sold to the grid. However, the selling price is way lower than the buying price, making the system lose financial efficiency.

Additionally, when the heat pump is introduced for these cities, other system size combinations emerge, as shown in Figure 4.8. In these situations, the electricity load is much higher due to the heat pump operation, and it becomes financially profitable to integrate the battery storage system with PV panels. The reason for this is the consumption coming from cooling during the summer, which did not play a significant role for Lisbon since the summers are milder than those in Cairo and Dakar.

4.3.1. Battery Price

As observed in the results, the battery storage system did not yield any financial profitability with the defined battery prices, leading to the absence of battery storage in the system configurations that resulted in the minimum NPC for each city. To explore the potential impact of anticipated future reductions in battery prices, an analysis was conducted to assess the effect of decreasing battery prices on NPC and system configuration. As outlined in Table 4.2, the battery cost was initially set at a fixed 600€ with a variable cost of 550€ per kWh. In contrast, the NPC analyses were conducted with a fixed cost of 550€ and a variable cost of 450€, a conservative approach still considering the expected decrease in future prices [6]. The results of the analysis with cheaper BESS can be found in Table B.1.

Amsterdam's system size remains unchanged with the battery becomes more affordable, as explained in section 4.3. However, when examining the system sizes that result in the minimum NPC for Lisbon, not only does the size of the BESS change, but the PV size also adjusts with the battery size. This serves as a notable illustration of how the sizes of system components mutually influence each other. By comparing the SSR for Lisbon in both Table 4.4 and Table B.1, an increase in SSR is evident. This indicates that the battery reduces grid dependency, allowing for a larger PV system and resulting in a lower NPC.

Table 4.5: Results of the system configurations with cheaper BESS.

	PV(kWp)	BSSS(kWh)	HP(kW)	NPC(€)	SCR	SSR
Amsterdam	0	0	4.5	41003	-	-
Lisbon	3.14	3	3	25646	0.49	0.67
Cairo	1.08	0	0	19675	0.57	0.44
	2.16	4	1	24345	0.87	0.77
Dakar	1.08	2.5	0	14890	0.95	0.81
	2.16	4	0.5	20463	0.75	0.92

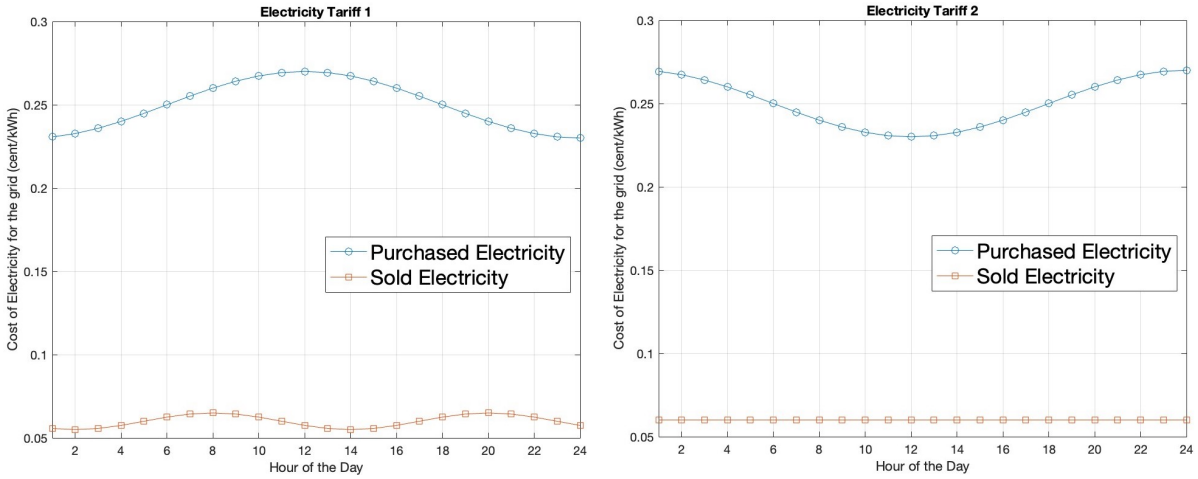

(a) Tariff 1. **(b)** Tariff 2

Figure 4.9: Different electricity tariffs.

For Cairo, the change in the battery price only leads to a slightly larger battery capacity in the heat pump size-forced scenario. However, the change in battery price has a considerable impact on Dakar. Examining the first system size for Dakar in Table B.1, the system reaches the minimum NPC with a 2.5 kWh battery storage, almost matching the price of the base scenario. Checking the SCR and SSR, one can observe that the battery makes the system not only more grid-independent with a 0.75 SCR but also retains the energy produced by the PV system, avoiding a loss of financial efficiency by selling it at a cheaper price to the grid with 0.92 SSR.

4.3.2. Electricity tariff

The electricity tariff utilized in section 4.3 was a generic tariff yielding results specific to the NPC and system configurations for each city. However, each country typically has a distinct tariff for purchased and sold electricity. The trend of the tariff has a direct impact on the NPC calculations as it affects the annual electricity cost term in Equation 4.5. To gauge the effect of the electricity tariff on the final system size decision, different tariff combinations should be tested for each city to assess the corresponding NPCs. While doing that, the BESS kept as the first prices to see the effect of the change of the electricity tariff trend only.

In the first electricity tariff, the purchased cost of electricity peaks during noon and reaches a minimum during the night. The price of electricity sold to the grid peaks at 8 am and 8 pm. In the new tariff to be tested, the average prices for both purchased and sold costs remain the same. However, for purchased electricity, it now peaks during the night, and for sold electricity, it remains constant at the average rate at all times. The tariffs can be seen in Figure 4.9.

The results of the change of the electricity tariff can be observed in Table 4.6. The base scenario results with that electricity tariff are similar to the one in Figure 4.6, only slightly lower for each city since the electricity bill goes 496€ from 505€ annually.

Table 4.6: Results of the system configuration with different electricity tariff.

	PV(kWp)	BSSS(kWh)	HP(kW)	NPC(€)	SCR	SSR
Amsterdam	0	0	4.5	40274	-	-
Lisbon	3.14	3	3	26183	0.49	0.67
Cairo	2.16	2.5	0	19940	0.57	0.87
	3.24	5	1	24302	0.7	0.91
Dakar	2.16	3	0	15249	0.57	0.98
	2.16	3.5	0.5	20967	0.72	0.9

While examining Amsterdam, no change can be observed for the system size that results in the minimum NPC. However, in the case of Lisbon, a change in the electricity tariff significantly impacts the system size. This change causes the battery size to increase from 0 to 3 kWh and the PV size from 2.16 kWp to 3.14 kWp. Lisbon experiences significant cooling demand during the winter.

In Tariff 1, it was more cost-effective to source electricity consumption for the heat pump from the grid, given the lower electricity prices during the night. However, with a change in the trend, it becomes financially more efficient to meet the demand using energy stored in the battery. The reason Amsterdam couldn't benefit from this tariff change is that it lacks substantial PV energy production during the day, unlike Lisbon, where excess energy can be stored for nighttime use. Consequently, battery technology is not advantageous for Amsterdam, when it is for Lisbon.

When examining Cairo and Dakar, a similar trend in the change of the system size is observed for both cities. With the transition from electricity tariff 1 to tariff 2, integrating BESS becomes beneficial for both locations. Under tariff 1, when there is no specified heat pump size for either city, having BESS was not financially attractive. However, with tariff 2 the BESS becomes financially appealing. Additionally, this tariff change leads to an increase in PV size due to the increase in battery sizes. In these cities, there is more PV production when electrical consumption is higher during the day. However, since the electricity price rises during the night when there is no PV production, it becomes more financially efficient to charge the batteries with excess energy and avoid drawing energy from the grid during the night when prices are higher. This trend is further evident in the high SSR ratios with tariff 2 for these cities.

The final system configurations that give the minimum NPC for each scenario are summarized in Figure 4.10, and compared with the base scenario defined in Figure 4.6.

Having conducted an economic analysis for each city, considering the system's entire lifetime, it is beneficial to examine the daily behavior of the system. This allows for a better understanding of the practical application of the integration model and reinforces the arguments presented regarding the trends in system configuration observed in NPC calculations. To achieve this, the daily trend of the optimal system scenario, determined with the consideration of discounted battery prices, is presented for Lisbon over four days of the year. This presentation aims to showcase the system's behavior across different seasons. The daily trends for Lisbon are illustrated in Figure 4.11.

Examining the components of the integrated system individually, starting with electricity consumption, one observes peaks during winter due to the seasonal heating operation of the heat pump and daily peaks during daylight hours. Analyzing the trend of AC power produced by the solar panels reveals summer peaks in both quantity and duration. Even in December, PV production remains at a decent level. In the daily trend across all seasons, the solar power production aligns well with electricity consumption, fostering self-consumption during all seasons except summer, and achieving self-sufficiency throughout the year. The system minimizes the need to purchase energy from the grid, especially during summer.

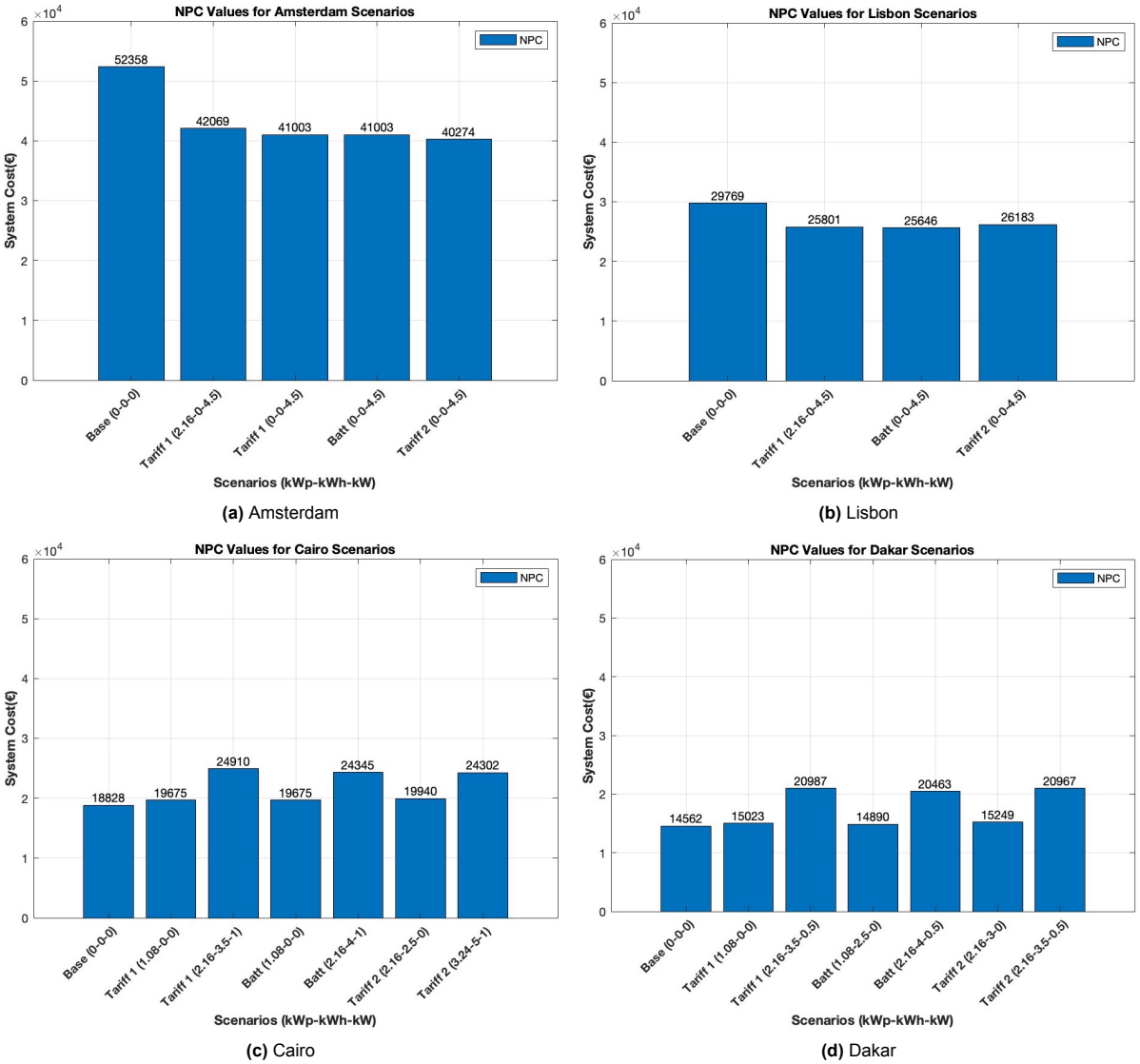

(a) Amsterdam **(b)** Lisbon

(c) Cairo **(d)** Dakar

Figure 4.10: Minimum NPC configuration for each city with for every scenario.

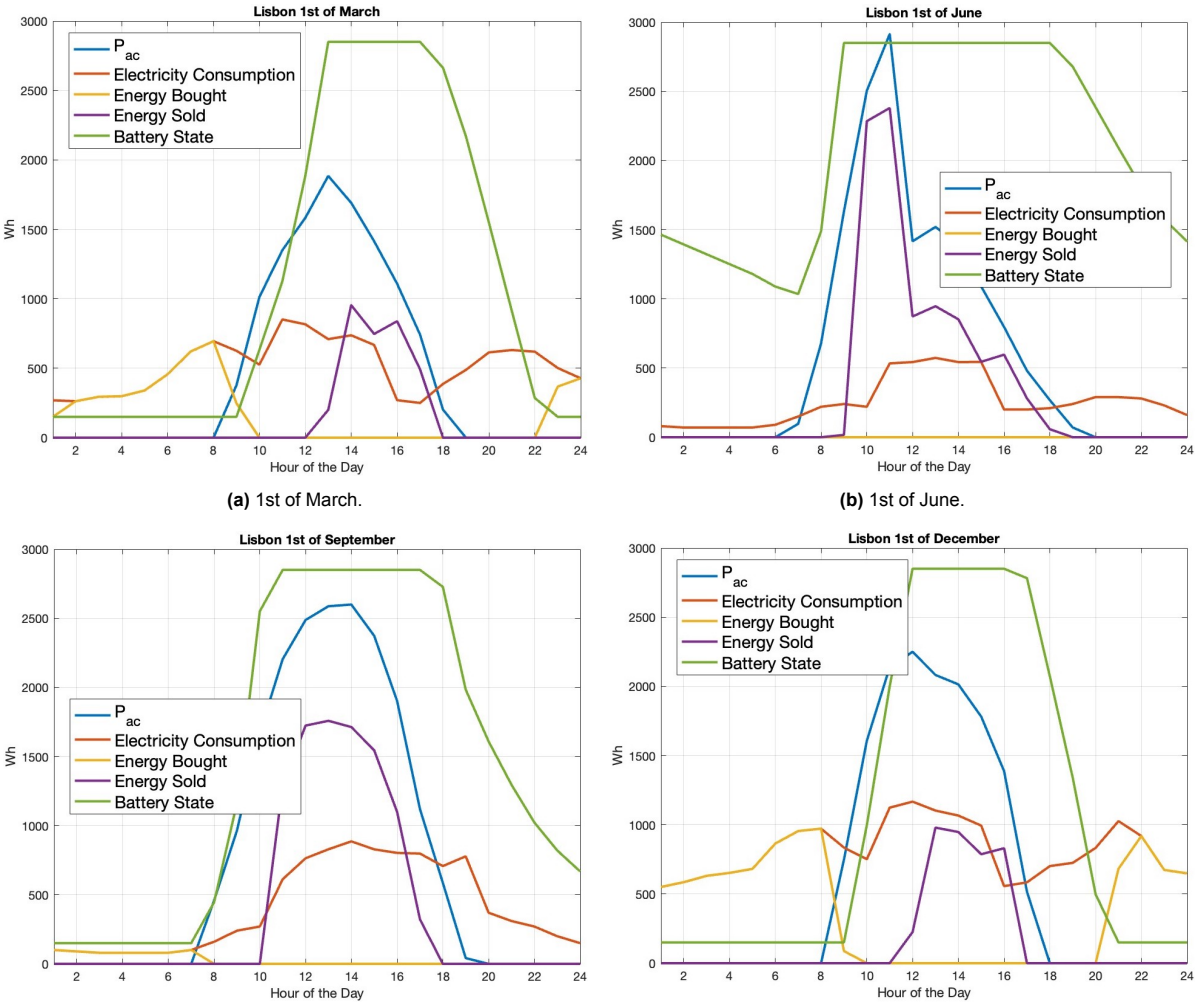

(a) 1st of March.

(b) 1st of June.

(c) 1st of September

(d) 1st of December.

Figure 4.11: Daily behaviour of the 3.18kWp PV-3 kWh BESS and 3 kW heat pump system for different days of the year in Lisbon .

Due to the city's matching demand and supply of electricity profiles, the system derives greater benefits from the Battery Energy Storage System (BESS), contributing to increased self-consumption and self-sufficiency. The battery actively engages in charging and discharging activities, rather than remaining idle or fully depleted for extended periods. This observation indicates a well-integrated system.

4.4. Conclusion

In conclusion, this chapter has successfully addressed the primary objective outlined in 'Sub-goal 3' that was 'Optimizing the energy systems by considering technical and economical aspects for different locations using the PVMD Toolbox'. The objective was to select various locations with different weather and climate conditions to analyze the integration model both economically and technically. The aim was to reach optimal system configurations by understanding how the model responds to different environmental factors.

Intentionally choosing cities with varied ESH, daylight hours, and temperatures aims to capture diverse energy production and consumption patterns. This deliberate selection facilitates comprehensive analyses, providing a deep understanding of integrated systems in different environmental contexts.

The initial heat pump analysis underscores that the economic viability of investing in a heat pump is heavily tied to the distinctive heating and cooling needs of a city. Cities with higher heating demands demonstrate a quick payback period, enhancing the appeal of heat pump investments. Conversely, in cities where cooling needs prevail, the economic rationale for a heat pump is less compelling, resulting in a considerably longer payback period since there is no operational cost change calculated coming from the cooling.

Finally, it has been determined that achieving financially optimal sizing requires consideration of multiple system factors, including initial investment costs and electricity tariffs, in conjunction with environmental factors. In cities where heating demand prevails during winter, installing a heat pump yields obvious financial benefits. If the cities have significant PV production, integrating PV with a heat pump provides even greater economic advantages. The integration of Battery Energy Storage Systems (BESS) into the system is strongly influenced by the initial investment cost of the technology and electricity tariffs. However, when it becomes financially appealing, it enables the inclusion of a larger PV size and enhances the system's self-sufficiency. For cities dominated by cooling demand, employing all three technologies results in a high-performance system with high SSR and SCR. Although the NPC for these cities exceeds the operational cost of the base scenario, it is important to note that the operational cost change for cooling is not considered in the calculations.

5

Conclusion and Future Work

This final chapter aims to provide the conclusion of the study and suggest future steps to advance the current research. Firstly, the study's conclusion will be presented, highlighting the most significant outcomes. Subsequently, recommendations will be provided for future endeavors related to this study.

5.1. Conclusion

The objective of this thesis defined in subsection 1.5.2 and stated as:

Designing and optimizing the energy systems of residential buildings in various cities with PV, heat pump and battery storage technologies by adding new features to the PVMD Toolbox.

To fulfill the main goal, sub-goals are formulated to systematically achieve the thesis objective. Each sub-goal contributes to the outcomes of the preceding step, progressively building toward the next stage.

Sub-goal 1: Integrating a heat pump model in PVMD Toolbox.

The first sub-goal is to create models for space heating, space cooling, and domestic hot water functions. These models should account for the respective demands associated with each purpose and calculate the corresponding electricity consumption.

To determine the most suitable modeling approach for integrating heat pumps into the overall framework of the study, a thorough exploration of various methods, including equation-fit and deterministic models, was conducted. Two specific models were selected for calculating COP and EER, aligning with the study's objectives. Interrelationships among COP, EER, and power requirements are explained with emphasizing their significance in assessing the energy efficiency of heat pump systems. Additionally, the methodology for acquiring essential input data for the models, such as heating and cooling demand and the use of the nPro tool, is explained.

Sub-goal 2: Integrating a battery model and building the integration of each component in PVMD Toolbox.

chapter 3 focused on modeling battery performance and integrating each component to observe their collective efficiency in a grid-connected energy system. Choosing a mathematical modeling approach aligned with the model's objectives accurately represented the battery's performance, based on literature review insights. The integration process systematically incorporated each component into the entire system. The previously developed heat pump model was integrated with household electricity consumption. Subsequently, the AC output from the PVMD toolbox was acquired and integrated into the model alongside the battery using AC coupling. This integration facilitated grid connection, culmi-

nating in the creation of a fully integrated system. This model enables the analysis of each component's performance across various locations throughout the year by providing location-specific inputs.

Sub-goal 3: Optimizing the energy systems by considering technical and economical aspects for different locations using the PVMD Toolbox.

The intentional selection of cities with diverse ESH, daylight hours, and temperatures serves to capture a wide range of energy production and consumption patterns. This purposeful variety facilitates thorough analyses, providing a profound insight into integrated systems across different environmental contexts. The initial heat pump analysis underscores the strong connection between the economic viability of heat pump investments and a city's unique heating and cooling demands. Cities with higher heating needs exhibit a rapid payback period, increasing the attractiveness of heat pump investments. In contrast, in cities dominated by cooling needs, the economic justification for heat pumps is less compelling, resulting in a significantly longer payback period.

Lastly, the determination for achieving financially optimal sizing involves considering multiple system factors, including initial investment costs and electricity tariffs, alongside environmental factors. For cities with predominant heating demands during winter, installing a heat pump yields evident financial benefits. Integration of PV with a heat pump offers greater economic advantages in cities with significant PV production. The inclusion of BESS is influenced by initial investment costs and electricity tariffs, and when financially viable, it allows for a larger PV size, enhancing system self-sufficiency. In cooling-dominated cities, employing all three technologies results in a high-performance system with high SSR and SCR. Although the NPC for these cities exceeds the operational cost of the base scenario, it was essential to note that the operational cost change for cooling is not considered in the calculations.

5.2. Future Work

There is always room for improvement in the study, which can bring it closer to real-life conditions and enhance its depth. This section will highlight the potential improvements that can be made to both the model and the corresponding analysis.

As mentioned in chapter 2, to incorporate the heating, cooling, and plug load demands of the household, nPro is utilized as an external toolbox. For this study, the demand data is directly received and integrated into the heat pump model. Looking forward, to reduce dependency on an external toolbox, these demands can be modeled within the PVMD toolbox. This involves assuming the structure of a generic house and utilizing heat transfer coefficients for walls and windows. Additionally, generic plug load consumption can be created for a household.

After creating heat pump models for air-to-water heat pumps and ground-source heat pumps to serve space heating, cooling, and domestic hot water purposes, the integrated analysis in chapter 4 focuses exclusively on air source heat pumps. This limitation is attributed to time constraints and the absence of a developed financial market for ground-source heat pumps. To observe the impact of higher COP values, understand their influence on electrical consumption, and evaluate their effects on system integration with other components, a similar analysis can be conducted for ground source heat pumps.

As mentioned in chapter 2, a simplified approach is adopted for domestic hot water. In reality, a buffer tank is required in the household to retain heated water and supply it as needed. However, in the model, the energy for domestic hot water demand is concentrated and supplied during a specific period of the day, considering the daily total demand for that purpose. Introducing a simple buffer tank model would enhance this domestic hot water approach, bringing it closer to its real-life application.

To obtain the AC output of the PV panels, several assumptions are made to simplify the model in terms of practicality. With these assumptions, the PV system is modeled as if it were in an open field, with panels exhibiting periodic properties. To align more closely with real-life applications of residential PV panels, the PV output can be generated using non-periodic properties, and creating generic horizons

for the locations to be analyzed.

The heat pump model operates based on calculating the COP by assessing the temperature difference between the source and the sink sides. By integrating the source side of the heat pump with Photovoltaic Thermal (PVT) panels, the performance of both the PVT panels and the heat pump can be analyzed, and the associated benefits can be observed. This integration introduces another dimension to the overall integrated system by incorporating PVT panels. Additionally, thermal storage can be introduced to further enhance the model, integrating it with both PVT panels and providing a more comprehensive approach for the domestic hot water purposes of the house. Consequently, the heat pump model can be seamlessly integrated with PVT and thermal storage models.

For the NPC calculations, the system is analyzed over a 20-year period. However, the degradation of solar panels and batteries is not included in the calculations. It is assumed that the performance of solar panels and batteries remains constant each year for the entire 20 years. To enhance the accuracy of the system performance and achieve more realistic NPC values, degradation models can be introduced for both PV panels and lithium-ion batteries.

References

[1] Ehsanolah Assareh et al. “Techno-economic analysis of combined cooling, heating, and power (CCHP) system integrated with multiple renewable energy sources and energy storage units”. In: Energy and Buildings 278 (2023), p. 112618.

[2] Christoph Beck et al. “Characterizing global climate change by means of Köppen climate classification”. In: Klimastatusbericht 51 (2005), pp. 139–149.

[3] T Beck et al. “Optimal operation, configuration and sizing of generation and storage technologies for residential heat pump systems in the spotlight of self-consumption of photovoltaic electricity”. In: Applied Energy 188 (2017), pp. 604–619.

[4] Mitul Ranjan Chakraborty et al. “A comparative review on energy storage systems and their application in deregulated systems”. In: Batteries 8.9 (2022), p. 124.

[5] Alessandro Ciocia et al. “Self-Consumption and self-sufficiency in photovoltaic systems: Effect of grid limitation and storage installation”. In: Energies 14.6 (2021), p. 1591.

[6] Wesley J Cole and Allister Frazier. Cost projections for utility-scale battery storage. Tech. rep. National Renewable Energy Lab.(NREL), Golden, CO (United States), 2019.

[7] Hongyuan Ding et al. “A safe reinforcement learning approach for multi-energy management of smart home”. In: Electric Power Systems Research 210 (2022), p. 108120.

[8] Energy.gov. Heat Pump Systems. 2021. URL: https://www.energy.gov/energysaver/heat-pump-systems (visited on 03/28/2022).

[9] Eurostat. Natural gas price statistics. 2024. URL: https://ec.europa.eu/eurostat/statistics-explained/index.php?title=Natural_gas_price_statistics#Natural_gas_prices_for_household_consumers (visited on 01/09/2024).

[10] Government of Canada. Heating and Cooling With a Heat Pump. 2022. URL: https://natural-resources.canada.ca/energy-efficiency/energy-star-canada/about/energy-star-announcements/publications/heating-and-cooling-heat-pump/6817 (visited on 03/28/2022).

[11] Holger C Hesse et al. “Economic optimization of component sizing for residential battery storage systems”. In: Energies 10.7 (2017), p. 835.

[12] Science Learning Hub. Heat pumps and energy transfer. 2014. URL: https://www.sciencelearn.org.nz/resources/241-heat-pumps-and-energy-transfer (visited on 04/06/2022).

[13] Dharani Kolantla et al. “Critical review on various inverter topologies for PV system architectures”. In: IET Renewable Power Generation 14.17 (2020), pp. 3418–3438.

[14] Lissy Langer and Thomas Volling. “A reinforcement learning approach to home energy management for modulating heat pumps and photovoltaic systems”. In: Applied Energy 327 (2022), p. 120020.

[15] Hong Li, Liangliang Sun, and Yonggui Zhang. “Performance investigation of a combined solar thermal heat pump heating system”. In: Applied Thermal Engineering 71.1 (2014), pp. 460–468.

[16] Yuanyuan Li et al. “Electrification of residential heating, cooling and hot water: Load smoothing using onsite photovoltaics, heat pump and thermal batteries”. In: Journal of Energy Storage 56 (2022), p. 105873.

[17] Daniele LIBERTO. Straight Line Basis Calculation Explained, With Example. 2024. URL: https://www.investopedia.com/terms/s/straightlinebasis.asp (visited on 01/09/2024).

[18] Meteonorm. Handbook part II: Theory. English. Version 8.2. Meteonorm. July 1, 2023. 84 pp. July 1, 2023.

[19] Sameh Monna et al. “A comparative assessment for the potential energy production from PV installation on residential buildings”. In: Sustainability 12.24 (2020), p. 10344.

[20] Georgios A Mouzeviris and Konstantinos T Papakostas. “Comparative analysis of air-to-water and ground source heat pumps performances”. In: International Journal of Sustainable Energy 40.1 (2021), pp. 69–84.

[21] Francesco Nicoletti, Mario Antonio Cucumo, and Natale Arcuri. “Cost optimal sizing of photovoltaic-battery system and air–water heat pump in the Mediterranean area”. In: Energy Conversion and Management 270 (2022), p. 116274.

[22] Pavlos Nikolaidis and Andreas Poullikkas. “A comparative review of electrical energy storage systems for better sustainability”. In: Journal of power technologies (2017).

[23] nPro About nPro. https://www.npro.energy/main/en/about-npro. Accessed: 2023-09-12.

[24] nPro DHW. https://www.npro.energy/main/en/load-profiles/heating/domestic-hot-water. Accessed: 2023-09-12.

[25] nPro Space Heating. https://www.npro.energy/main/en/load-profiles/heating/space-heating. Accessed: 2023-09-12.

[26] Eric O’Shaughnessy et al. “Solar plus: Optimization of distributed solar PV through battery storage and dispatchable load in residential buildings”. In: Applied Energy 213 (2018), pp. 11–21.

[27] Antonella Priarone, Federico Silenzi, and Marco Fossa. “Modelling heat pumps with variable EER and COP in energyplus: A case study applied to ground source and heat recovery heat pump systems”. In: Energies 13.4 (2020), p. 794.

[28] Neelam Rathore et al. “A comprehensive review of different types of solar photovoltaic cells and their applications”. In: International Journal of Ambient Energy 42.10 (2021), pp. 1200–1217.

[29] Sergi Obrador Rey et al. “Powering the future: a comprehensive review of battery energy storage systems”. In: Energies 16.17 (2023), p. 6344.

[30] Arthur Rinaldi et al. “Decarbonising heat with optimal PV and storage investments: A detailed sector coupling modelling framework with flexible heat pump operation”. In: Applied Energy 282 (2021), p. 116110.

[31] Oliver Ruhnau, Lion Hirth, and Aaron Praktiknjo. “Time series of heat demand and heat pump efficiency for energy system modeling”. In: Scientific data 6.1 (2019), p. 189.

[32] Graziano Salvalai. “Implementation and validation of simplified heat pump model in IDA-ICE energy simulation environment”. In: Energy and Buildings 49 (2012), pp. 132–141.

[33] Monika Sandelic, Ariya Sangwongwanich, and Frede Blaabjerg. “Reliability evaluation of PV systems with integrated battery energy storage systems: DC-coupled and AC-coupled configurations”. In: Electronics 8.9 (2019), p. 1059.

[34] Marderos Ara Sayegh et al. “Heat pump placement, connection and operational modes in European district heating”. In: Energy and Buildings 166 (2018), pp. 122–144.

[35] Masoume Shabani et al. “Techno-economic impacts of battery performance models and control strategies on optimal design of a grid-connected PV system”. In: Energy Conversion and Management 245 (2021), p. 114617.

[36] Arno Smets et al. Solar Energy:The physics and engineering of photovoltaic conversion, technologies and system Bloomsbury Publishing, 2016.

[37] George Stamatellos, Olympia Zogou, and Anastassios Stamatelos. “Interaction of a house’s rooftop PV system with an electric vehicle’s battery storage and air source heat pump”. In: Solar. Vol. 2. 2. MDPI. 2022, pp. 186–214.

[38] Brandon R Sutherland. “Solar materials find their band gap”. In: Joule 4.5 (2020), pp. 984–985.

[39] Javier Uche et al. “A Sustainable Polygeneration System for a Residential Building”. In: Applied Sciences 12.24 (2022), p. 12992.

[40] MR Vogt et al. “Introducing a comprehensive physics-based modelling framework for tandem and other PV systems”. In: Solar Energy Materials and Solar Cells 247 (2022), p. 111944.

[41] Tetsuya Wakui et al. “Predictive management for energy supply networks using photovoltaics, heat pumps, and battery by two-stage stochastic programming and rule-based control”. In: Energy 179 (2019), pp. 1302–1319.

[42] Zheng Wang et al. “State of the Art on Heat Pumps for Residential Buildings”. In: Buildings 11 (Aug. 2021), p. 350. DOI: 10.3390/buildings11080350.

[43] Zhiqiang Zhai et al. “ENERGY STORAGE FOR RESIDENTIAL BUILDINGS: REVIEW AND ADVANCES”. In: Jan. 2013.

[44] Yaning Zhang et al. “Application of an air source heat pump (ASHP) for heating in Harbin, the coldest provincial capital of China”. In: Energy and Buildings 138 (2017), pp. 96–103.

[45] Shenghua Zou and Xiaokai Xie. “Simplified model for coefficient of performance calculation of surface water source heat pump”. In: Applied Thermal Engineering 112 (2017), pp. 201–207.

A

Validation of Heat Pump Models

Ruhnau et al [31]. calculated the the equation-fit models for three type of heat pumps using the manufacturer data performing quadratic regression and can be seen in Figure A.1.

Mouzeviris and Papakostas [20] calculated the the equation-fit models for ASHP and GSHP using the manufacturer data performing quadratic regression and can be seen in Figure A.2. and Figure A.3.

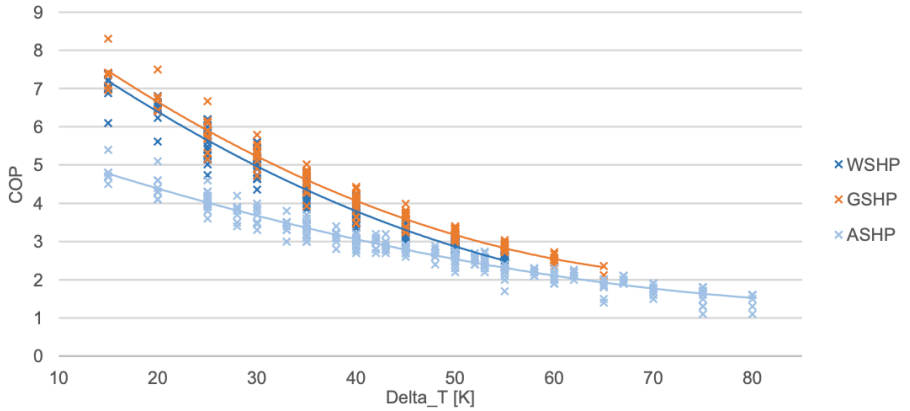

Figure A.1: Performed quadratic regression to evaluate the equation fits of different type of heat pumps for heating with respect to the available manufacturer data [31].

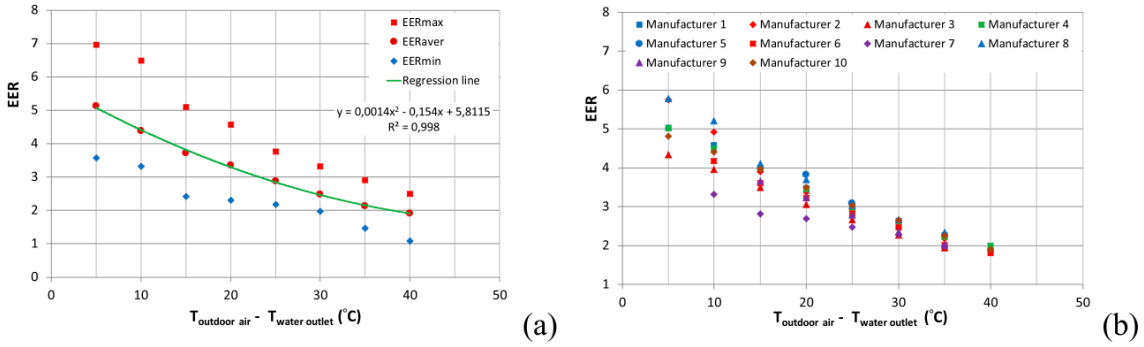

Figure A.2: Performed quadratic regression to evaluate the equation fits of ASHP for cooling with respect to the available manufacturer data [20].

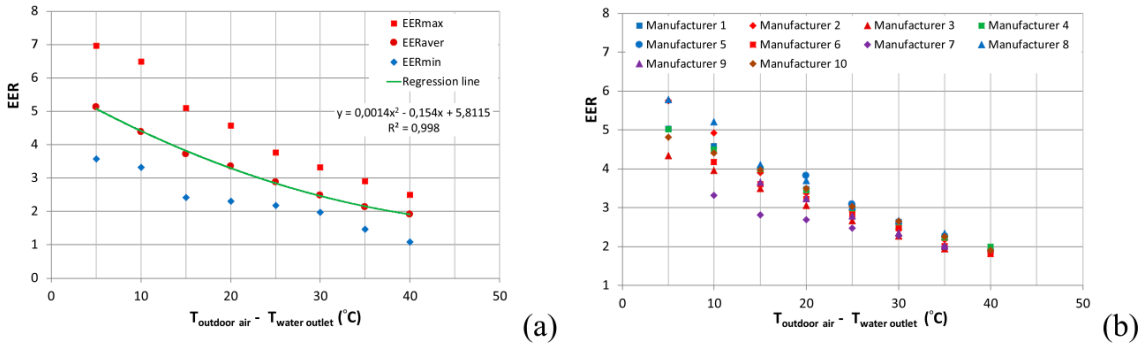

Figure A.3: Performed quadratic regression to evaluate the equation fits of GSHP for cooling with respect to the available manufacturer data [20].

B

Specifications of the PV panel and the string inverter

Table B.1: Parameters of inverter used.

	Vac	Paco	Pdco	Vdco	Pso	C0	C1
ABB: PVI 3.0	V	W	W	V	W	1/W	1/V
OUTD-S-US-Z-M-A	240	3000	3125,758	340,8429	19,86611	-6,66E-06	-2,55E-05
(240 V) 240V	**C2**	**C3**	**Pnt**	**Vdcmax**	**Idcmax**	**Mppt_low**	**Mppt_high**
[CEC 2014]	1/V	1/V	W	V	A	V	V
	1,05E-03	-4,71E-04	0,1	600	20	160	530

ELECTRICAL PARAMETERS

TYPE	STKM-60-270
Rated Maximum Power at STC (Wp)	270
Open Circuit Voltage (Voc/V)	38.40
Maximum Power Voltage (Vmp/V)	31.15
Short Circuit Current (Isc/A)	8.97
Maximum Power Current (Imp/A)	8.51
Module Efficiency [%]	18.20
Power Tolerance	0+3%
Temperature Coefficient of Isc (αIsc)	+0.05%/°C
Temperature Coefficient of Voc (βVoc)	-0.34%/°C
Temperature Coefficient of Pmax (γPmp)	-0.42%/°C
STC Irradiance 1000W/m², Module Temperature 25°C, AM 1.5	

Produced according to IEC 61215:2005, IEC 61730:2004 standard

Figure B.1: Data sheet of the PV panel used in the analysis.

C

NPC Plots of the cities

C.1. Battery Analysis

The results of the NPC contour plots for optimized scenarios with the decreased battery price.

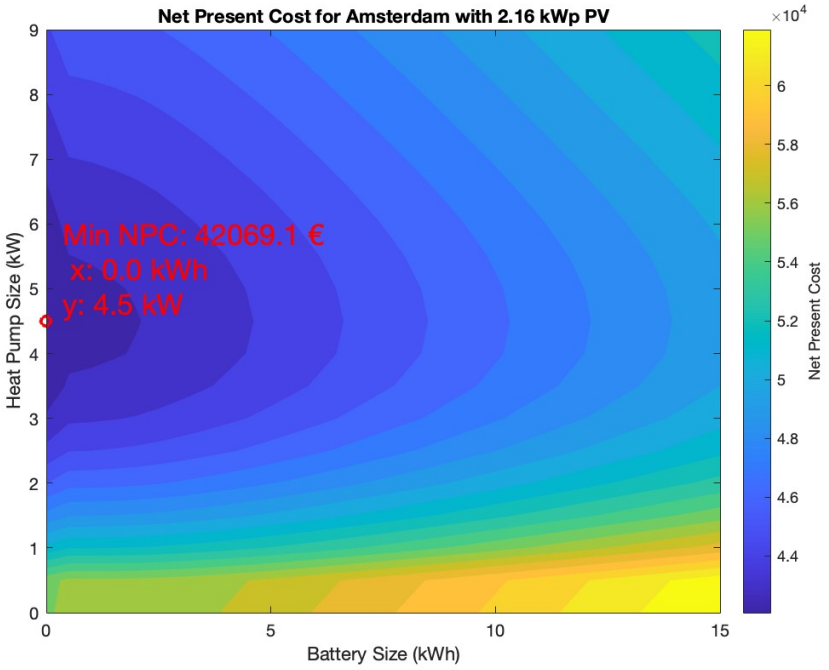

Figure C.1: Amsterdam.

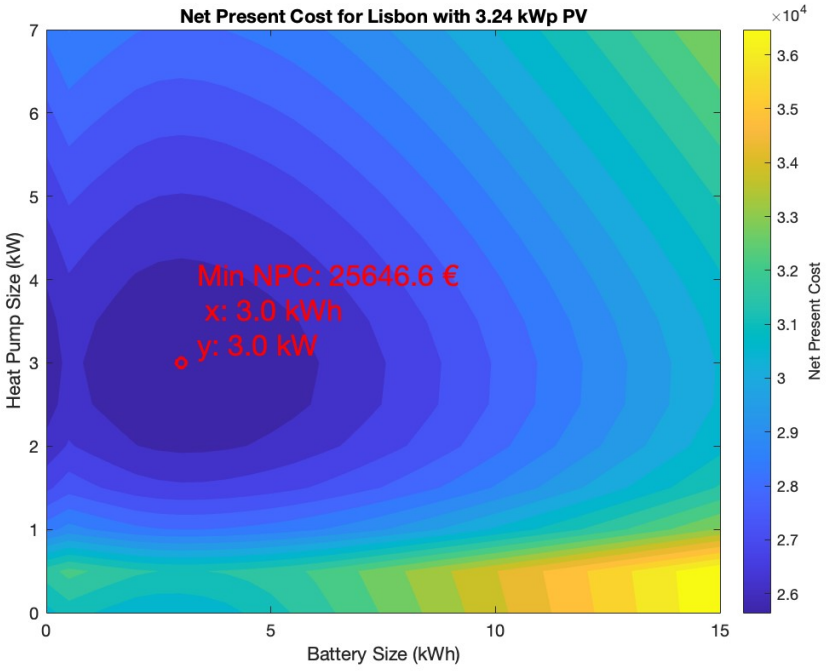

Figure C.2: Lisbon.

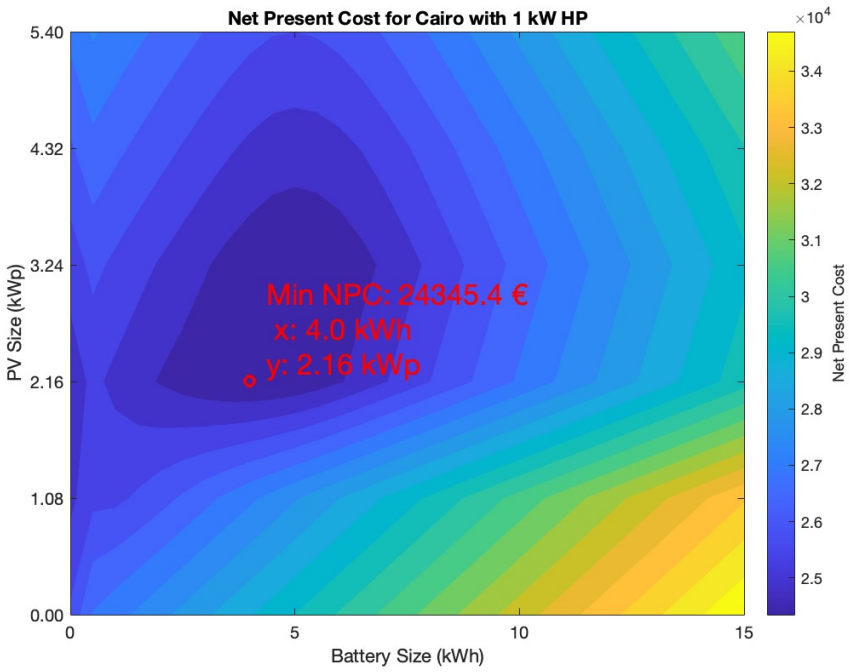

Figure C.3: Cairo.

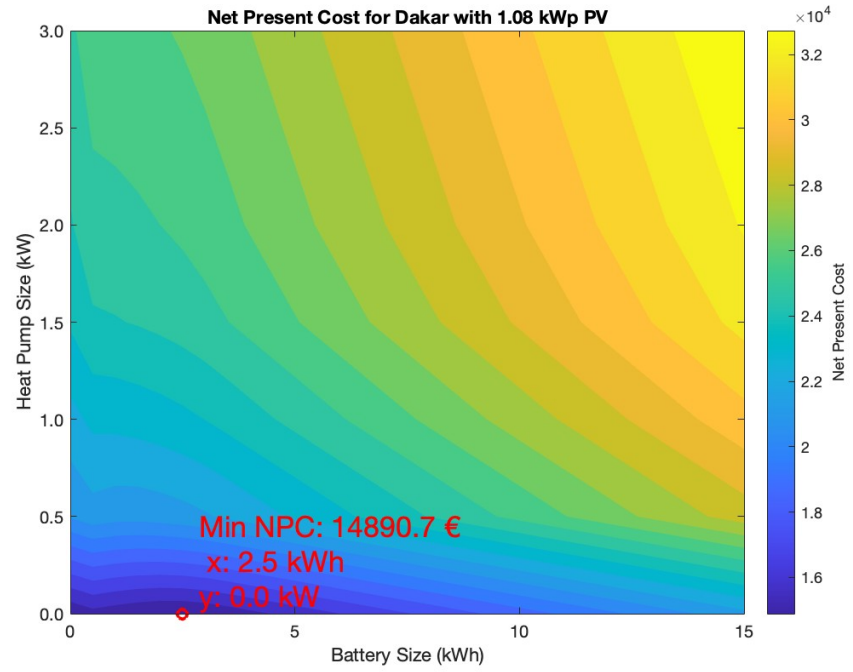

Figure C.4: Dakar.

C.2. Electricity Tariff Analysis

The results of the NPC contour plots for optimized scenarios with the changed electricity tariff.

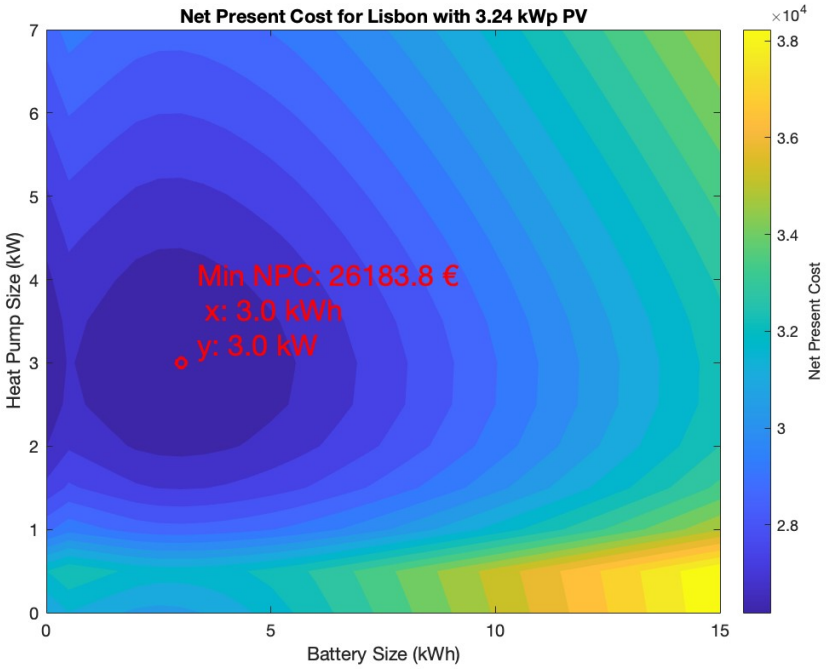

Figure C.5: Lisbon.

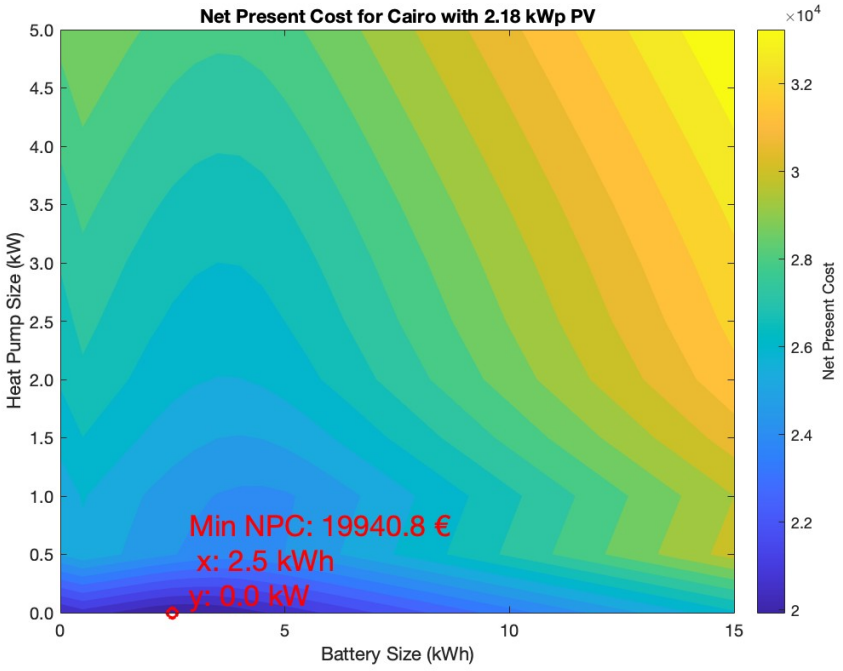

Figure C.6: Cairo.

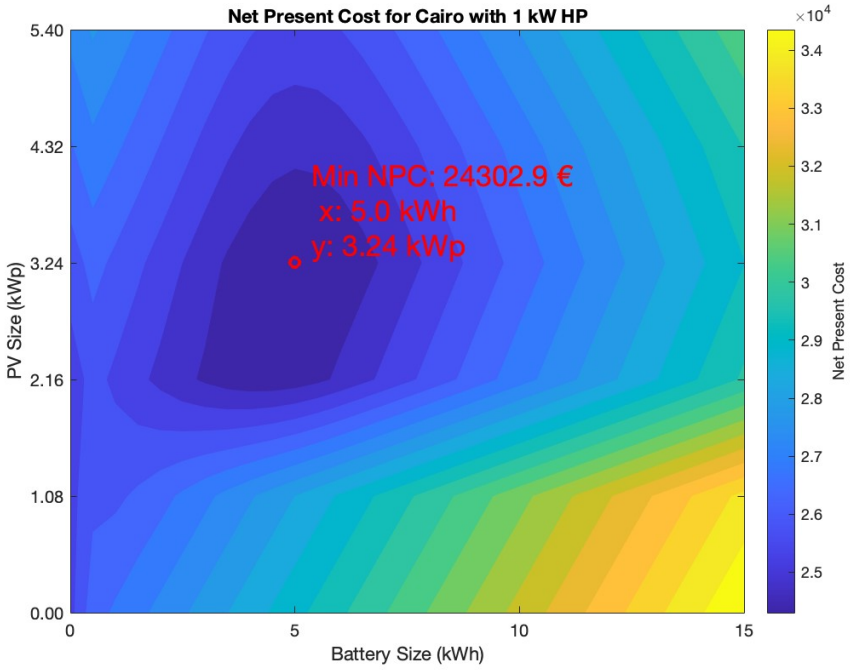

Figure C.7: Cairo.

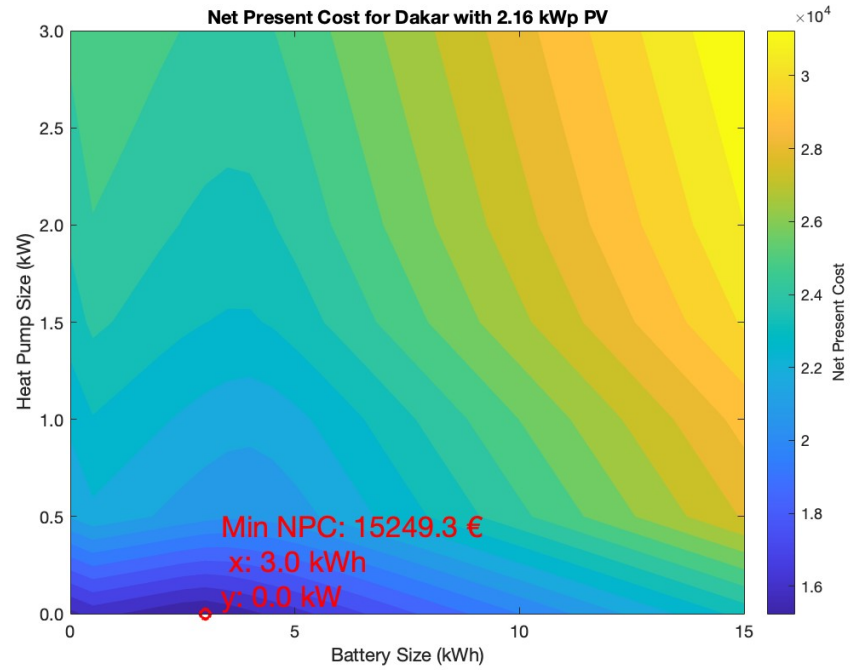

Figure C.8: Dakar.

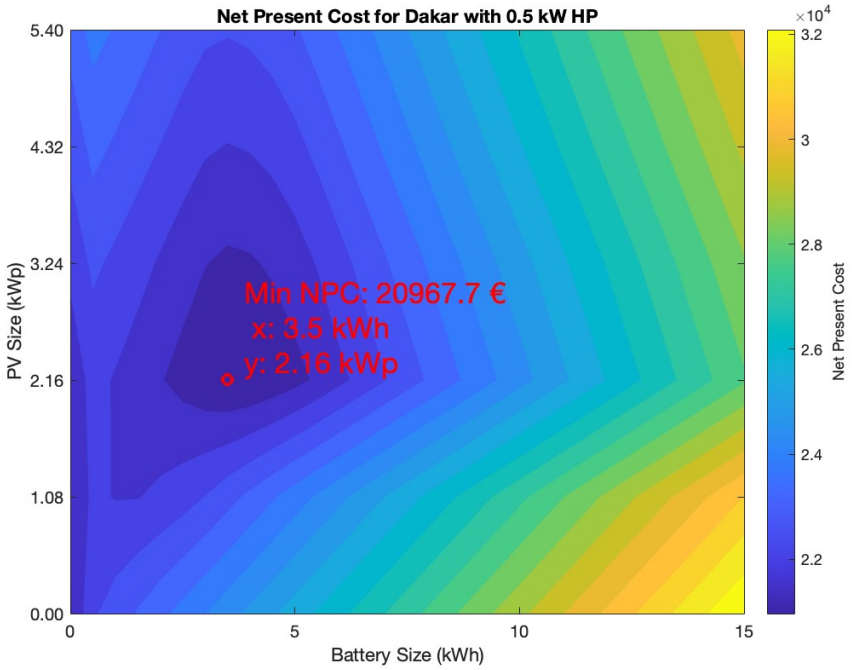

Figure C.9: Dakar.